Title: Activating mutations in genes related to TCR signaling in angioimmunoblastic and other follicular helper T-cell-derived lymphomas.
Authors: Vallois D, Dobay MP, Morin RD, Lemonnier F, Missiaglia E, Juilland M, Iwaszkiewicz J, Fataccioli V, Bisig B, Roberti A, Grewal J, Bruneau J, Fabiani B, Martin A, Bonnet C, Michielin O, Jais JP, Figeac M, Bernard OA, Delorenzi M, Haioun C, Tournilhac O, Thome M, Gascoyne RD, Gaulard P, de Leval L
Journal: Blood
Year: 2016 Sep 15
Volume: 128
Issue: 11
Pages: 1490-502
DOI: 10.1182/blood-2016-02-698977

Activating mutations in genes related to TCR signaling in angioimmunoblastic and other follicular helper T-cell-derived lymphomas

David Vallois[1*], Maria Pamela D. Dobay[2*], Ryan D. Morin[3,4], François Lemonnier[5], Edoardo Missiaglia[1], Mélanie Juilland[6], Justyna Iwaszkiewicz[2], Virginie Fataccioli[5], Bettina Bisig[1], Annalisa Roberti[1], Jasleen Grewal[3], Julie Bruneau[7], Bettina Fabiani[8], Antoine Martin[9], Christophe Bonnet[10], Olivier Michielin[2,17], Jean-Philippe Jais[11], Martin Figeac[12], Olivier A. Bernard[13], Mauro Delorenzi[2], Corinne Haioun[14], Olivier Tournilhac[15], Margot Thome[6], Randy D. Gascoyne[16], Philippe Gaulard[5#] and Laurence de Leval[1#].

[1] Institute of Pathology, Centre Hospitalier Universitaire Vaudois, Lausanne, Switzerland

[2]SIB Swiss Institute of Bioinformatics, University of Lausanne, Lausanne, Switzerland

[3]Department of Molecular Biology and Biochemistry, Simon Fraser University, Burnaby, BC, Canada

[4]Genome Sciences Centre, BC Cancer Agency, Vancouver, BC, Canada

[5]INSERM U955, Université Paris-Est, Hôpital Henri-Mondor, Département de Pathologie, Créteil, France

[6]Department of Biochemistry, University of Lausanne, Lausanne, Switzerland

[7]Service d'Anatomie et cytologie pathologiques, Hopital Necker, Paris, France

[8]Service d'Anatomie et cytologie pathologiques, Hopital Saint-Antoine, Paris, France

[9]Service d'Anatomie pathologique, Hopital Avicenne, Bobigny, France

[10]Hématologie clinique, CHU Liège, Belgique

[11]Service de Biostatistiques, GH Necker Enfants malades, Paris, France

[12]Plate-forme de Génomique Fonctionnelle et Structurale, Institut Pour la Recherche sur le Cancer de Lille, Lille, France

[13]INSERM U1170, Institut Gustave Roussy, Villejuif, France

[14]Hémopathies lymphoides, CHU Henri Mondor, Creteil, France

[15]Hématologie Clinique, CHU Estaing, Clermont-Ferrand, France

[16]Centre for Lymphoid Cancer, BC Cancer Agency, Vancouver, BC, Canada

[17]Centre Hospitalier Universitaire Vaudois, Oncology, Lausanne, Switzerland

[*]co-first authors

[#]co-last authors

Running title: Mutation-induced TCR activation in TFH nodal PTCL

Keywords: T-cell lymphoma, Angioimmunoblastic, TCR signaling, next generation sequencing, activating mutations

Scientific category: Lymphoid neoplasia

Corresponding author: Pr. Laurence de Leval ; **mailing adress:** CHUV Institut de Pathologie, Rue du Bugnon 25, 1011 Lausanne Switzerland ; **phone:** +41 (0)21 314 71 94 ; **FAX:** +41 (0)21 314 72 05 ; **e-mail:** Laurence.deLeval@chuv.ch

Word count (abstract): 233

Word count (main text): 3993

Table(s) count: 1

Figure(s) count: 7

References count: 58

Key points

- A high frequency of diverse, activating mutations in co-stimulatory/TCR-related signaling genes occur in AITL and other TFH-derived PTCL
- Deregulated TCR activation may play a role in the pathogenesis of TFH-derived PTCL, paving the way for developing novel targeted therapies

Abstract

Angioimmunoblastic T-cell lymphoma (AITL) and other lymphomas derived from follicular T-helper cells (TFH) represent a large proportion of peripheral T-cell lymphomas (PTCL) with poorly understood pathogenesis and unfavorable treatment results. We investigated a series of 85 patients with AITL (n=72) or other TFH-derived PTCL (n=13) by targeted deep sequencing of a gene panel enriched in T-cell receptor (TCR) signaling elements. *RHOA* mutations were identified in 51/85 cases (60%) consisting of the highly recurrent dominant negative G17V variant in most cases and a novel K18N in 3 cases, the latter showing activating properties in *in vitro* assays. Moreover, half of the patients carried virtually mutually exclusive mutations in other TCR-related genes, most frequently in *PLCG1* (14.1%), *CD28* (9.4%, exclusively in AITL), *PI3K* elements (7%), *CTNNB1* (6%) and *GTF2I* (6%). By *in vitro* assays in transfected cells, we demonstrated that 9/10 PLCG1 and 3/3 CARD11 variants induced MALT1 protease activity and increased transcription from NFAT or NF-kB response element reporters, respectively. Collectively, the vast majority of variants in TCR-related genes could be classified as gain-of-function. Accordingly, the samples with mutations in TCR-related genes other than *RHOA* had transcriptomic profiles enriched in signatures reflecting higher T-cell activation. Although no correlation with presenting clinical features nor significant impact on survival was observed , the presence of TCR-related mutations correlated with early disease progression. Thus, targeting of TCR-related events may hold promise for the treatment of TFH-derived lymphomas.

Introduction

Angioimmunoblastic T-cell lymphoma (AITL), one of the most common peripheral T-cell lymphomas (PTCL)[1,2] comprises CD4-positive neoplastic T cells with a T follicular helper (TFH) immunophenotype, and an important reactive microenvironment[3]. Additionally, a subset of PTCL not otherwise specified (PTCL-NOS) exhibiting a TFH-like immunophenotype and overlapping characteristics with AITL, are believed to be part of the same disease spectrum [4,5]. The prognosis of AITL remains poor, with a 5-year overall survival of around 30% [1,6]. Although autologous stem cell transplantation may improve the response to conventional first-line therapy, early disease progression makes it frequently impossible [7]. Thus, pinpointing new druggable targets for developing specific therapies in TFH-derived lymphomas remains critical.

Recurrent mutations in the epigenetic regulators *TET2*, *IDH2* and *DNMT3A* have been detected in AITL and TFH-like PTCLs [8,9], but are not likely sufficient to drive lymphomagenesis[10,11]. A highly recurrent dominant-negative G17V mutation in the RHOA GTPase was recently discovered in up to 70% of AITL and TFH-like PTCLs [12-14]. RHOA is activated downstream of T-cell receptor (TCR) engagement in mature T cells and is linked to cytoskeleton reorganization following T-cell activation [12,13]. Although their exact role in human T-cell transformation remains uncertain, *RHOA* mutations tend to co-occur with *TET2* mutations, suggesting that they represent a second event in multistep AITL lymphomagenesis[15]. Finally, AITL also bears a variety of other less recurrent genetic alterations[12,13,16].

In B-cell lymphomas, constitutive B-cell receptor (BCR) signaling via somatic mutation-induced or antigen-mediated activation of key BCR components lead to neoplastic B-cell survival and expansion[17]. Several lines of evidence suggest that TCR activation might be similarly relevant to PTCL pathogenesis. For example, NPM1-ALK chimeric proteins induce an

intracellular cascade of events substituting to TCR signaling in anaplastic large cell lymphoma [18]. The *ITK-SYK* fusion present in rare PTCLs likewise drives lymphomagenesis by triggering antigen-independent activation of TCR signaling pathways in mice[19]. Mutations or gene fusions in co-stimulatory/TCR signaling genes as *CD28, FYN, PLCG1* or *CARD11* have also been reported in several PTCLs[12,20-25]. However, alterations in the TCR signaling pathway have not yet been extensively studied in TFH-related lymphomas. Here, we focused on investigating mutations in the co-stimulatory/TCR signaling cascade in a series of AITL and TFH-like PTCLs using a targeted deep sequencing approach. Besides frequent RHOA mutations, we demonstrated recurrent activating and virtually mutually exclusive mutations in co-stimulatory/TCR pathway components in 49% of the cases. Notably, we found several mutations in *PLCG1* and *CARD11* that we characterized as functionally activating *in vitro*. Integrated analysis with gene expression profiles indicated that TCR-mutated samples were enriched for molecular signatures reflecting higher T-cell activation and proliferation. Clinically, TCR-mutated patients receiving anthracyclin-based chemotherapy showed an increased early progression risk compared to patients without such mutations. These results indicate the potential of using drugs that reduce TCR signaling for treating these lymphomas.

Methods

Patients and Tumor Samples

Discovery cohort: eleven paired tumoral and normal samples from 10 clinically annotated AITL patients were subject to whole-genome (WGS, n=8) or whole-exome sequencing (WES, n=3) (**Table S1**).

Extended cohort: targeted deep sequencing (TDS) was performed on DNA extracted from frozen tissue biopsies of an extended cohort of 85 previously untreated patients (72 AITL and 13 TFH-like PTCL-NOS). In three patients, paired samples were analyzed. These cases and associated clinical annotations (**Table S2**), were collected in the framework of the Tenomic LYSA consortium. Diagnoses were confirmed by expert hematopathologists. Criteria used to define TFH-like PTCL, NOS were previously reported [8]. A subset of these patients were analysed for *TET2*, *IDH2* and *DNMT3A* mutations in previous studies[8,9] The study was approved by the local ethics committee (CPP Ile de France IX 08-009).

WGS, WES and TDS

Libraries were constructed for WGS following a standard protocol[26]. 100-bp paired-end reads were generated using an Illumina HiSeq 2000 Sequencer (version 3 chemistry). Reads were mapped to the NCBI Build 36.1 reference genome using the Burrows-Wheeler Aligner (BWA) alignment tool version 0.5.7, algorithm aln. PCR duplicates were eliminated using Picard version 1.38. Indels and Single Nucleotide Variants (SNVs) were called using Strelka version 1.0.14, removing false positive calls internally. Variants were independently identified for each tumor-

germline pair, using the germline as reference. GRCh37 coordinates of the filtered indels and SNVs were obtained using LiftOverVCF. Variants were annotated with VEP, and their read counts were obtained using in-house scripts. Copy Number Variations (CNVs) were identified using HMMcopy. Commonly deleted or amplified regions from WGS were visually identified using the Integrative Genome Viewer Software (IGV, https://www.broadinstitute.org/igv/). Deleted loci and genes having SNVs and/or CNVs in at least two patients are listed in **Tables S3 and S4**.

TDS of sixty-nine genes (**Table S5**) was performed on the extended cohort. Systematic sequencing errors were removed by adding two randomly selected blood samples from four healthy volunteers to each run. Libraries were prepared using the True-Seq Custom Amplicon kit (Illumina) and sequenced on a MiSeq machine (Illumina, 1000x mean depth, mean coverage 94%). Variants were called using MiSeq reporter using default settings and were visually inspected on IGV. All synonymous variants and known SNPs with an allelic frequency above 0.1% in public databases (dbSNP131, 1000 Genomes Project, 5000 Exomes project) were filtered out. We excluded variants found in normal samples, in ambiguously mapped regions from captured pseudogenes, and in regions of low complexity. Candidate variants were independently validated in a second round of TDS: we selectively amplified the amplicons covering the positions of candidate mutations (IonAmpliseq kit, Lifetechnologies) and sequenced them on a Ion PGM System (Lifetechnologies; 1305x mean depth, mean coverage 91.64%). Variants were called using default settings of the IonReporter software and reviewed with IGV. The final variants list (**Table S6**) was generated applying the following flitering criteria: a) variants called by both platforms, b) variants with minor allele frequency (MAF) < 0.4, c) variants already described as somatic in the COSMIC database. Filter b) was introduced to take

in to account the low tumor content and the inavaillability of matched normal samples. The threshold was defined based on the Minor Allelic Frequency (MAF) range of well-characterized AITL mutations, such as in *RHOA* and *CD28*[12-14,25]. Variants were annotated using GeneTalk (http://www.**gene-talk**.de/).

Cloning and Functional validation

A detailed description is provided in supplemental material. Briefly, we performed site-directed mutagenesis of *RHOA*, *PLCG1* and *CARD11* mutations on cloned cDNAs into pcMV6-MycFlag (*RHOA, PLCG1*) (Origene, C terminal tag) and pcDNA3-HA (*CARD11*) (N terminal tag)[27] vectors. RHOA variants were functionally assessed *in vitro* with rhotekin pull-down assays[12-14] and SRE (Serum Responsive Element) (Promega, Madison, WI, USA) luciferase reporter assay using HEK293T cells

PLCG1 and CARD11 variants were functionally tested by fluorescence resonance energy transfer (FRET)-based determination of their ability to induce MALT1 protease activity in HEK293T cells [28] and in luciferase-based assays using a NFAT reporter in HEK293T cells (forPLCG1) or a NF-B reporter in Jurkat cells deficient in *CARD11*[29] (kindly provided by Dr. Xin Lin) (for CARD11) .

Western blot analysis

The following primary antibodies were used in Western blotting: anti-HA (Covalab Biotechnology), anti-Myc (clone 4A6, Millipore), anti-CARD11 (clone 1D12, Cell Signaling), anti-MALT1 [28] and anti-Actin (ab3280, Abcam). Secondary antibodies were purchased from Jackson Laboratories.

Gene expression and enrichment analysis

Gene expression profiles generated by hybridization on Affymetrix U133 Plus 2.0 were available for the extended cohort[3]. Rotation testing using mean ranks (ROMER, R package limma) was used to determine the gene set signature enrichments in TCR_Mut compared to TCR_WT patients. A total of 304 signatures, including 23/50 hallmark signatures and nine signatures from the curated and immunogenic signature collection of the Molecular Signatures Database (MSigDB, http://software.broadinstitute.org/gsea/msigdb), all signatures of interest in lymphoid biology (Staudt, lymphochip.nih.gov/signaturedb/) and two manually annotated sequences linked to TCR signaling, were tested.

Clinical correlations and survival analysis

Frequency differences of categorial variables were analyzed using Fisher's exact test, while differences in continuous variables were tested with the Wilcoxon rank sum test. Overall survival (OS) was defined as time from diagnosis to death or last follow up, while progression free survival (PFS) was defined as time from treatment initiation to death or progression or last follow up. Analyses of OS and PFS were performed using the Kaplan-Meier method and hazard ratio differences were computed with the log rank test.

Results

Whole exome/genome sequencing reveals alterations in T-cell signaling genes in AITL

Eleven tumor samples from 10 AITL patients were subject to WGS or WES and compared to germline DNA (**Figure S1 and Table S1**). On average, 91% of the genome had >10× coverage, with 68% having >30×. A mean of 27 single nucleotide variations (SNV) per patient (range: 11-50) was observed in coding regions, except in a sample from a relapsing patient with a chromothripsis pattern of structural variation (**Figure S2**) and 225 SNVs. In one patient refractory to first-line therapy, WGS performed on tumor biopsies at diagnosis and after 5 cycles of chemotherapy, revealed a similar profile of alterations, with identical *TET2* and *ANKRD62* SNVs in both samples. CNV analysis revealed multiple loci deleted in a number of patients, with eight minimal common regions (**Table S3**), mostly in three patients. A total of 39 genes had SNVs and/or CNVs in at least two patients (**Table S4**). Apart from *RHOA* G17V and *TET2* mutations, 9/39 (23%) altered genes were related to TCR (n=7), Toll-like receptor (n=1) or Wnt (n=1) signalings. Other mutations were found in genes involved in the cell cycle (n=5), autophagy (n=2), or other pathways (n=6). Six additional genes relevant to TCR or JAK/STAT signaling (*CTNNB1, VAV1, MTOR, CREBBP, PIK3C2G, JAK1*) were altered in one patient each. Collectively, T-cell signaling alterations were found in 7/10 patients.

Frequent mutations of *RHOA* and other TCR-related genes are confirmed in an extended cohort of TFH-derived lymphomas

We designed a panel of 69 genes for TDS, partly based on findings in the discovery cohort **(Tables S5 and Figure S1**), for application on our extended cohort (**Table S2**). After orthogonal cross-validation and conservative filtering (**Table S6** and **Figure S3)** we validated 70 variants in 29 genes (**Figure 1**), including missenses (61), frameshifts (5), non-frameshift deletions (2), and

stop-gain mutations (2)**.** Mutations were detected in 70/85 samples (82%, mean mutations per sample = 1.8). *RHOA* and other TCR signaling-related genes accounted for 19 of 29 (65.5%) mutated genes (**Figures 1 and 2**).

RHOA mutations include a novel activating K18N variant

RHOA was the most frequently mutated gene among those analyzed (51/85; 60% patients), with a similar prevalence in AITL and TFH-like PTCL. Consistent with previous reports[12,13], the G17V variant was found in most of the cases. We also identified a novel K18N mutation (VF: [5.5%; 7.4%; 10%]) in three AITL patients (**Figure 3A and Table 1**). Both mutations occur in the highly conserved GTP binding site of RHOA. We tested Myc-tagged G14V (constitutively active[30]), G17V (dominant negative), K18N as well as WT RHOA in a pull-down assay using Rhotekin-RBD (Rho Binding Domain) beads (**Figure 3B**). While RHOA G17V already characterized as dominant negative[12-14] did not bind RBD beads even in the presence of FBS as compared to WT, RHOA K18N showed a marked increase of RBD beads binding similarly to RHOA G14V (Figure 3B). Moreover, unlike RHOA G17V that did not activate and even repressed transcription from the SRE under serum activation, RHOA K18N markedly enhanced its transcription (**Figure 3C**).

Mutations in other TCR signaling-related genes are variably recurrent and diverse

Apart from *RHOA*, mutations in genes involved in TCR costimulation or signaling were detected in 42/85 patients (49%) (**Figures 1-2 and Table 1**).

CD28 and TCR-proximal signaling genes

Three different *CD28* mutations, T195P, D124V and D124E, all described previously[13,25,31] were identified in 4, 2 and 2 AITL patients, respectively (8/85, 9.4%) (**Figure 4A**). All TFH-like

PTCL were *CD28*-WT. T195P and D124V mutations are known to enhance TCR/CD28-induced NF-kB activity *in vitro* [25,31]. Three patients (2 AITL, 1 TFH-like PTCL; 3.5%) harbored mutations in *FYN*, a TCR- and CD28-proximal kinase component (**Figure 4B**). Mutations in the SH2 domain (S186L) and the absence of phosphorylated tyrosine 531 (T524fs or Q527X mutations) probably confer enhanced kinase activity by disrupting their inhibitory interaction [12]. The two amino acid substitution in the tyrosine kinase domain of LCK observed in one AITL patient is expected to enhance its kinase activity [32]. We did not find mutations in *ICOS, ZAP70, LAT* or *ITK*.

NF-kappaB/NFAT pathway

Ten different-missense mutations spanning the coding region of *PLCG1* (VF: [2.1%; 38%]) were identified in 12/85 patients (8 AITL, 4 TFH-like PTCL; 14.1%) (**Figure 5A**). Apart from previously reported variants in Adult T-cell Leukemia/Lymphoma (ATLL) or in other PTCL[20-24], we identified two novel variants (E730K and G869E). We generated all mutant constructs and tested their activity against WT PLCG1 in a FRET-based reporter assay of MALT1 protease activity[27,28] (**Figure 5B**) and in a NFAT luciferase reporter assay (**Figure 5C**). Both experiments confirmed that the S345F and S520F variants were activating [21]. All six variants in the PI-PLC, SH2, SH3 and C2 domains were also activating, increasing the FRET signal by 1.7 to 3-fold and the luciferase expression by 4 to 5-fold. Of the two PH1 domain variants, R48W had no effect in both assays, while E47K increased NFAT reporter activity by 2.1 fold and FRET signal by 1.5-fold.

Point mutations in *CARD11*, which encodes a scaffolding protein downstream of PLCG1 required for CD28/TCR-induced NF-kB activation [28] were found in two AITL and one TFH-like

PTCL (3.5%). The F176C variant affects the coiled-coil domain of the protein, commonly mutated in DLBCL [33]. The S547T and F902C variants map to linker regions with undefined structure (**Figure 5D**). In a FRET-based assay[28], F176C and S547T enhanced MALT1 proteolytic activity by 2- and 4-fold, respectively, while the F902C mutant, previously reported in ATLL patients [20], had no detectable effect (**Figure 5E**). When transfected into Jurkat cells deficient for *CARD11*[29], we found that, compared to wildtype CARD11, all three variants induced enhanced NF-kB reporter activity in response to PMA/Ionomycin stimulation (**Figure 5F**).

PI3K pathway

Six patients (3 AITL, 3 TFH-like PTCL; 7%) showed mutations in *PI3K* genes encoding the regulatory subunits PIK3R1 (n=5), PIK3R5 (n=1) or the catalytic subunit PIK3CA (n=1) (**Figure 4C-E**). These mutations likely enhance the catalytic subunit activity or increase PIK3R1 binding to CD28 [34]. Five AITL patients (5.9%) had mutations in *PDPK1* (PDK1), a master serine/threonine kinase with multiple targets including AKT**.** Three missense mutations were found on or near its kinase domain, suggesting an activating effect[35] (**Figure 4F**). Four different *CTNNB1* mutations, known to occur in a variety of carcinomas and Wilms tumors, were identified in five patients (4 AITL, 1 TFH-like PTCL; 5.9%) (**Figure 4G**). All have been previously characterized as activating or stabilizing variants that induce persistent signaling and increased proliferation, and have been linked to both poor treatment response and frequent tumor relapse in various tumors[36,37].

AP-1/MAPK pathway

Eleven patients (8 AITL, 3 TFH-like PTCL; 13%) had mutually exclusive activating mutations in the MAPK pathway, which regulate the activity of the AP-1 transcription factor family. Activating *KRAS* [38] and *STAT3*[26,39] mutations were detected in three and two patients each (**Figure 4H**). We also found five missense mutations in *GTF2I* (*TFII-I*) [40], (**Figure 4I**) that are likely activating, as those reported in thymic epithelial tumors [41].

GTPases pathway

Apart from highly recurrent *RHOA* mutations, four patients (3 AITL, 1 TFH-like PTCL; 4.7%) harbored previously undescribed frameshift deletions or missense mutations in *VAV1*, a guanosine exchange factor for RAC1, CDC42 and RHOA (**Figure 4J**). Two missense mutations were on the second SH3 domain, where a D797 residue mutation was previously shown to activate VAV1-mediated transformation via cell-cell contact deregulation [42].

Analysis of sequential biopsies

Analysis of paired samples in four refractory or relapsed patients (**Table S8**) showed that the mutations identified at diagnosis were also present in the second biopsy, with overall very similar VF. Within the limit of the panel of genes examined, two patients presented one additional mutation at relapse (*CTNNB1* and *VAV1*), at somewhat lower VF than those present at diagnosis. Although this analysis is limited to a few pairs of samples, it indicates that the mutational heterogeneity that characterizes many AITL samples appears to be preserved and essentially not modified by the treatments administered.

Activating mutations in TCR signaling-related genes correlate with molecular signatures reflecting higher T-cell activation and with response to therapy

A total of 66/85 patients harbored mutations in TCR signaling genes. To assess the biological and clinical impact of the tumor mutational status, we focused on patients with mutations in TCR signaling-related genes other than *RHOA*, designated hereafter as "TCR_Mut" (42/85 cases, 49%), and compared them to those with only *RHOA*, or no detectable mutation, designated "TCR_WT" (43/85 cases, 51%). (**Figure 6**).

Mutations in TCR-related genes other than *RHOA* were virtually non-overlapping, and the vast majority (47/56 distinct variants, 84%) were either functionally validated (n=24) or predicted (n=23) to be biologically gain-of-function mutants (**Figure 6**). Consequently, nearly all TCR_Mut patients (39/42 patients, 93%) harbored at least one activating mutation.

There was no significantly differentially expressed genes between TCR_Mut and TCR_WT samples (**Figure S4**). However, the molecular signatures of TCR_Mut were significantly enriched in fifteen gene sets compared to TCR_WT by enrichment analysis (**Figure 7A, Table S7, Figure S5**), reflecting the activation of signaling pathways like PI3K, NF-kB[17], IRF4, JAK-STAT, as well as the upregulationof calcium signaling target genes. This points towards TCR signaling activation in TCR_Mut PTCLs. TCR_Mut samples also showed enrichment in cell cycle signatures reflecting increased proliferative activity. Finally, there was a trend for TCR_Mut samples to have downregulated proximal TCR signaling genes (signature "T_cell") such as TCR (*TCRα, TCRβ; CD3δ, CD3γ*), signaling molecules (*LAT, TRIM, SAP, FYB, ZAP70*) and cell surface markers (adjusted p. value = 0.10), a feature consistent with sustained T-cell activation [43].

Then, when comparing the clinical features and outcome of TCR_Mut and TCR_WT patients, no significant differences in main clinical characteristics at presentation (**Table S9**) or in overall survival (18 vs 40 months median OS; 5 year OS 20% vs 29%; p=0.37) were found (**Figure S6**). Strikingly, however, among the 59 patients (49 AITL and 10 TFH-like PTCLs) who received anthracyclin-based induction chemotherapy, 11/33 (33%) TCR_Mut patients versus 2/26 (8%) TCR_WT (p=0.02, **Table S9**) showed early progression, relapse or no response to treatment within the first six months after diagnosis. This, however, did not translate into a

statistically significant difference in progression-freee survival at 5 years (21% versus 24% for TCR_Mut versus TCR_WT patients, p=0.15) (**Figure 7B-C**).

Discussion

In this study, we confirmed the high prevalence of *RHOA* mutations in TFH-derived PTCL, with most samples bearing the dominant negative G17V variant. Interestingly, we identified a new K18N variant in 3% of the patients that presented activating features in *in vitro* assays. This intriguing finding of distinct *RHOA* mutations with apparently opposite functional properties in the same disease, was also recently documented in ATLL[44,45]. Further studies are warranted to understand how these variants may contribute to the pathogenesis of PTCLs.

Apart from *RHOA* alterations, we identified activating and virtually mutually exclusive mutations in diverse TCR signaling genes in half of TFH-derived lymphomas. Individually, the frequencies of these mutations were variable, with the five most mutated genes (*PLCG1, CD28, PIK3* elements, *GTF2I, CTNNB1)* being altered in 14% to 5% of the patients. *CD28* and *FYN* mutations in AITL were previously described in a small number of cases[12-14]. Our study significantly expands these previous results, and strongly supports a role of activated TCR signaling in the pathogenesis of TFH-derived PTCLs, drawing strong parallels with the role of BCR signaling in B-cell lymphomas.

Mutations in genes related to TCR co-stimulation and signaling were recently reported in other PTCL enties, like cutaneous T-cell lymphomas (CTCL), PTCL-NOS and ATLL[20-24,46]. Nonetheless, mutations in specific genes are variably recurrent in distinct entites [24,25], and for a given gene the distribution of the mutations and their relative prevalence are heterogeneous. For instance, *PLCG1* and *CARD11* mutations are highly prevalent (up to 18% and 15% of the cases, respectively) in CTCL, in which conversely *CD28* mutations are not found. [20] *CARD11* mutations are more frequent in ATLL (24%) and Sésary syndrome (SS, 10.9%) than in this series of TFH-derived lymphomas. Whether the observed mutations are sufficient to induce

constitutive activation of the respective pathways, and how their effect may be dependent or influenced by antigen-driven or other stimulatory signals remains unknown. Interestingly, some of the TCR-related genes may be altered through point mutations or small indels as well as by major structural rearrangements, amplifications and deletions[20,23,24]. Collectively, these findings strongly suggest that genetic alterations impacting TCR signaling operate as a common pathogenic mechanism in several PTCL entities.

Our analysis also explored the JAK/STAT and TLR pathways. Mutation-induced activation of the JAK/STAT pathway, highly prevalent in myeloid neoplasms, was recently identified as a major oncogenic mechanism in several T-cell leukemias and lymphomas derived from innate immune cells[20,46-53]. Our results suggest, however, that JAK/STAT mutations do not have the same importance in the pathogenesis of TFH-derived lymphomas, as only 4/85 patients bore a single activating mutation each in *JAK1, JAK2, JAK3* or *MYD88* (**Table 1**)[54]. Except for *JAK2* V617F, the three others were observed in *PLCG1*-mutated cases.

Our data further support that AITL and TFH-like PTCL are closely related at the molecular level[5], and share common oncogenic mechanisms. We and others have reported the occurrence of *TET2*, *DNMT3A* and *RHOA* mutations in a large proportion of both AITL and TFH-like PTCL patients[5,8,9,12-14]. This study extends the molecular overlap across TFH-derived neoplasms to genetic alterations in various TCR-signaling. Interestingly, *CD28* mutations were exclusively identified in AITL patients, consistent with recent reports[25,31]. Similarly, *IDH2* mutations were rarely detected in PTCL cases[9,55], suggesting that the distribution of some genetic features might be relevant in distinguishing AITL from other TFH-derived nodal lymphomas, which otherwise share many common features[5].

In the proposed multistep model of pathogenesis for TFH-derived PTCL, mutation-induced epigenetic deregulation, possibly arising in early hematopoietic precursors, may promote the emergence of premalignant cells, which requires additional genetic events to acquire a definitively malignant phenotype[13,56]. It has been thus suggested that *RHOA* alterations occur as a second event in *TET2* and/or *DNMT3A*-mutated cells[13,56,57]. The prevalence of mutations in *TET2*, *DNMT3A* and *IDH2* analyzed in a subset of our cases was 52% (34/65 cases), 29% (17/56 cases) and 30% (21/71 cases), respectively[8,9]. These mutations were not mutually exclusive, and in fact tended to co-occur with each other, as previously reported [12,13]. We also found a tendency for *RHOA* mutations to associate with epigenetic alterations, since *RHOA* mutations were detected in 31/41 (76%) cases mutated in *TET2*, *DNMT3A* and/or *IDH2*, but in only 8/23 (35%) cases without epigenetic mutations (p=0.003). Since the proportion of neoplastic cells in AITL is typically low and variable from case to case[3], the comparison of VF of different mutated genes was performed for each individual sample. In 13 cases harboring mutations in both *TET2* and/or *DNMT3*, and *RHOA* or *IDH2* with available VF, the *TET2/DNMT3A* VF was significantly higher than for *RHOA* or *IDH2* (**Figure S7A**). There was no obvious association of *RHOA* mutations with other TCR-related genes, as 27/51 (53%) *RHOA*-mutated and 15/34 (44%) *RHOA*-WT cases were mutated in other TCR-related genes (p=0.51). In twenty-seven cases mutated in both *RHOA* and one or several genes of the TCR, JAK/STAT or TLR pathways, no significant difference in VF means was observed between *RHOA* and other genes (**Figure S7B**).

Although our results warrant confirmation in cohorts of patients treated on prospective clinical trials, they suggest that the mutational status of TCR-related genes may have important clinical implications, predicting early treatment failure with anthracyclin-based chemotherapy in TFH-related PTCL patients. Importantly, several activating mutations found in PI3K or NFkB

pathways could be targeted by idelalisib or the proteasome inhibitor bortezomib, respectively. It is of interest to determine their efficacy in TCR_Mut patients[12,21], possibly in combination with demethylating agents[58]. Thus, similar to the importance of targeting BCR signaling in B-cell lymphomas with the BTK inhibitor ibrutinib[17], characterization of the TCR mutational status might open new avenues to design specific and hopefully more effective therapies. In clinical practice, given the high number of genes involved and the diversity of mutations found, targeted deep sequencing with high depth/coverage appears as the method of choice for selecting patients.

Acknowledgments

This work was supported by grants received from the Plan Cancer (Belgium), the Ligue du Cancer (Switzerland), the Institut National du Cancer (INCa AAP PLBIO13-085, INCa-DGOS 2010-085, and INCa-Plan Cancer 2013) and the MEDIC foundation.

We acknowledge Catherine Chapuis (Pathology, Lausanne) and Caroline Communaux from the LYSA-Pathology for their technical assistance.

We acknowledge K Harshman and the LGFT (Lausanne Genomic Technology Facility) for their technical support.

We acknowledge Céline Villenet et Sabine Quief from the plate-forme de génomique fonctionnelle et structurale, Lille University, for the WES experiments.

Authorship

Contribution: D. Vallois, R. Morin, M. Thome, R.D. Gascoyne, L. de Leval and P. Gaulard were involved in the conception and design of the study. D. Vallois, M.P. Dobay developed the methodologies. D. Vallois, M.P. Dobay, J. Bruneau, B. Fabiani, A. Martin, C. Bonnet, F. Lemonnier, M. Juilland, M Thome, J. Iwaszkiewicz, A. Roberti and B. Bisig acquired the data. D. Vallois, MP Dobay, E. Missiaglia, F. Lemonnier, M. Juilland, O. Michielin, O Tournilhac, C Haioun, M. Delorenzi, O. Bernard, J.P. Jais and J. Grewal analysed and interpreted the data. D. Vallois, M.P. Dobay, F. Lemonnier, E. Missiaglia, L. de Leval and P. Gaulard worte the manuscript. V. Fataccioli was the administrative, technical and material support. L. de Leval and P. Gaulard supervised the study.

Conflict-of-interest disclosure: the authors have no conflict of interest to disclose

Correspondence: Pr. Laurence de Leval, CHUV Institut de Pathologie, Rue du Bugnon 25, 1011 Lausanne, Switzerland; **e-mail:** Laurence.deLeval@chuv.ch

References

1. Federico M, Rudiger T, Bellei M, et al. Clinicopathologic characteristics of angioimmunoblastic T-cell lymphoma: analysis of the international peripheral T-cell lymphoma project. *J Clin Oncol.* 2013;31(2):240-246.

2. de Leval L, Parrens M, Le Bras F, et al. Angioimmunoblastic T-cell lymphoma is the most common T-cell lymphoma in two distinct French information data sets. *Haematologica.* 2015;100(9):e361-e364.

3. de Leval L, Rickman DS, Thielen C, et al. The gene expression profile of nodal peripheral T-cell lymphoma demonstrates a molecular link between angioimmunoblastic T-cell lymphoma (AITL) and follicular helper T (TFH) cells. *Blood.* 2007;109(11):4952-4963.

4. Gaulard P, de Leval L. Pathology of peripheral T-cell lymphomas: where do we stand? *Semin Hematol.* 2014;51(1):5-16.

5. Dobay MP LF, Missiaglia E, Bastard C, Vallois D, Jais JP, Fataccioli V, Scourzic L, Dupuy A, Martin-Garcia N, Parrens M, Le Bras F, Rousset T, Picquenot JM, Tournilhac O, Delarue R, Bernard O, Delorenzi M, de Leval L and Gaulard P. A PTCL, NOS subset with molecular and clinical features similar to AITL. *Hematological Oncology.* 2015;33(Issue supplement S1):100-180.

6. Mourad N, Mounier N, Briere J, et al. Clinical, biologic, and pathologic features in 157 patients with angioimmunoblastic T-cell lymphoma treated within the Groupe d'Etude des Lymphomes de l'Adulte (GELA) trials. *Blood.* 2008;111(9):4463-4470.

7. Corradini P, Vitolo U, Rambaldi A, et al. Intensified chemo-immunotherapy with or without stem cell transplantation in newly diagnosed patients with peripheral T-cell lymphoma. *Leukemia.* 2014;28(9):1885-1891.

8. Lemonnier F, Couronne L, Parrens M, et al. Recurrent TET2 mutations in peripheral T-cell lymphomas correlate with TFH-like features and adverse clinical parameters. *Blood.* 2012;120(7):1466-1469.

9. Cairns RA, Iqbal J, Lemonnier F, et al. IDH2 mutations are frequent in angioimmunoblastic T-cell lymphoma. *Blood.* 2012;119(8):1901-1903.

10. Jaiswal S, Fontanillas P, Flannick J, et al. Age-Related Clonal Hematopoiesis Associated with Adverse Outcomes. *N Engl J Med.* 2014;371(26):2488-2498.

11. Muto H, Sakata-Yanagimoto M, Nagae G, et al. Reduced TET2 function leads to T-cell lymphoma with follicular helper T-cell-like features in mice. *Blood Cancer Journal.* 2014;4(12):e264.

12. Palomero T, Couronne L, Khiabanian H, et al. Recurrent mutations in epigenetic regulators, RHOA and FYN kinase in peripheral T cell lymphomas. *Nat Genet.* 2014;46(2):166-170.

13. Sakata-Yanagimoto M, Enami T, Yoshida K, et al. Somatic RHOA mutation in angioimmunoblastic T cell lymphoma. *Nat Genet.* 2014;46(2):171-175.

14. Yoo HY, Sung MK, Lee SH, et al. A recurrent inactivating mutation in RHOA GTPase in angioimmunoblastic T cell lymphoma. *Nat Genet.* 2014;46(4):371-375.

15. Cleverley SC CP, SHenning SW and Cantrell DA. Loss of Rho function in the thymus is accompanied by the development of thymic lymphoma. *oncogene.* 2000;19(1):13-20.

16. Odejide O, Weigert O, Lane AA, et al. A targeted mutational landscape of angioimmunoblastic T-cell lymphoma. *Blood.* 2014;123(9):1293-1296.

17. Wilson WH, Young RM, Schmitz R, et al. Targeting B cell receptor signaling with ibrutinib in diffuse large B cell lymphoma. *Nat Med.* 2015;21(8):922-926.

18. Inghirami G, Chan WC, Pileri S, the AxcG-dtmolm. Peripheral T-cell and NK cell lymphoproliferative disorders: cell of origin, clinical and pathological implications. *Immunological Reviews.* 2015;263(1):124-159.

19. Pechloff K, Holch J, Ferch U, et al. The fusion kinase ITK-SYK mimics a T cell receptor signal and drives oncogenesis in conditional mouse models of peripheral T cell lymphoma. *J Exp Med.* 2010;207(5):1031-1044.

20. Kataoka K, Nagata Y, Kitanaka A, et al. Integrated molecular analysis of adult T cell leukemia/lymphoma. *Nat Genet.* 2015;47(11):1304-1315.

21. Vaque JP, Gomez-Lopez G, Monsalvez V, et al. PLCG1 mutations in cutaneous T-cell lymphomas. *Blood.* 2014;123(13):2034-2043.

22. Manso R, Rodríguez-Pinilla SM, González-Rincón J, et al. Recurrent presence of the PLCG1 S345F mutation in nodal peripheral T-cell lymphomas. *Haematologica.* 2015;100(1):e25-e27.

23. da Silva Almeida AC, Abate F, Khiabanian H, et al. The mutational landscape of cutaneous T cell lymphoma and Sezary syndrome. *Nat Genet.* 2015;47(12):1465-1470.

24. Wang L, Ni X, Covington KR, et al. Genomic profiling of Sezary syndrome identifies alterations of key T cell signaling and differentiation genes. *Nat Genet.* 2015;47(12):1426-1434.

25. Rohr J, Guo S, Huo J, et al. Recurrent activating mutations of CD28 in peripheral T-cell lymphomas. *Leukemia.* 2016;30(5):1062-1070.

26. Morin RD, Mendez-Lago M, Mungall AJ, et al. Frequent mutation of histone-modifying genes in non-Hodgkin lymphoma. *Nature.* 2011;476(7360):298-303.

27. Lenz G DR, Ngo Vu N, Lam L, George TC, Wright GW, Dave SS, Zhao H, Xu W, Rosenwald A, Ott G, Muller-Hermelink HK, Gascoyne RD, Connors JM, Rimsza LM, Campo E, Jaffe ES, Delabie J, Smeland EB, Fisher RI, Chan WC, Staudt LM. Oncogenic CARD11 Mutations in Human Diffuse Large B Cell Lymphoma. *Science.* 2008;319(5870):1676-1679.

28. Pelzer C, Cabalzar K, Wolf A, Gonzalez M, Lenz G, Thome M. The protease activity of the paracaspase MALT1 is controlled by monoubiquitination. *Nat Immunol.* 2013;14(4):337-345.

29. Wang D, You Y, Case SM, et al. A requirement for CARMA1 in TCR-induced NF-[kappa]B activation. *Nat Immunol.* 2002;3(9):830-835.

30. Ihara K, Muraguchi S, Kato M, et al. Crystal Structure of Human RhoA in a Dominantly Active Form Complexed with a GTP Analogue. *Journal of Biological Chemistry.* 1998;273(16):9656-9666.

31. Lee SH, Kim JS, Kim J, et al. A highly recurrent novel missense mutation in CD28 among angioimmunoblastic T-cell lymphoma patients. *Haematologica.* 2015;100(12):e505-507.

32. Lorraine E Laham NMaTMR. The activation loop in Lck regulates oncogenic potential by inhibiting basal kinase activity and restricting substrate specificity. *Oncogene.* 2000;19(35):3961-3970.

33. Lenz G, Davis RE, Ngo VN, et al. Oncogenic CARD11 Mutations in Human Diffuse Large B Cell Lymphoma. *Science.* 2008;319(5870):1676-1679.

34. Huang C-H, Mandelker D, Schmidt-Kittler O, et al. The Structure of a Human p110α/p85α Complex Elucidates the Effects of Oncogenic PI3Kα Mutations. *Science.* 2007;318(5857):1744-1748.

35. Chinen Y, Kuroda J, Shimura Y, et al. Phosphoinositide Protein Kinase PDPK1 Is a Crucial Cell Signaling Mediator in Multiple Myeloma. *Cancer Research.* 2014;74(24):7418-7429.

36. Austinat M, Dunsch R, Wittekind C, Tannapfel A, Gebhardt R, Gaunitz F. Correlation between β-catenin mutations and expression of Wnt-signaling target genes in hepatocellular carcinoma. *Molecular Cancer.* 2008;7(1):1-9.

37. Pilati C, Letouzé E, Nault J-C, et al. Genomic Profiling of Hepatocellular Adenomas Reveals Recurrent FRK-Activating Mutations and the Mechanisms of Malignant Transformation. *Cancer Cell.* 2014;25(4):428-441.

38. Stolze B, Reinhart S, Bulllinger L, Fröhling S, Scholl C. Comparative analysis of KRAS codon 12, 13, 18, 61, and 117 mutations using human MCF10A isogenic cell lines. *Scientific Reports.* 2015;5:8535.

39. Ohgami RS, Ma L, Monabati A, Zehnder JL, Arber DA. STAT3 mutations are present in aggressive B-cell lymphomas including a subset of diffuse large B-cell lymphomas with CD30 expression. *Haematologica.* 2014;99(7):e105-e105.

40. Sacristán C, Schattgen SA, Berg LJ, Bunnell SC, Roy AL, Rosenstein Y. Characterization of a novel interaction between transcription factor TFII-I and the inducible tyrosine kinase in T cells. *European Journal of Immunology.* 2009;39(9):2584-2595.

41. Petrini I, Meltzer PS, Kim I-K, et al. A specific missense mutation in GTF2I occurs at high frequency in thymic epithelial tumors. *Nat Genet.* 2014;46(8):844-849.

42. Razanadrakoto L, Cormier F, Laurienté V, et al. Mutation of Vav1 adaptor region reveals a new oncogenic activation. *Oncotarget.* 2015;6(4):2524-2537.

43. Singh NJ, Schwartz RH. The Strength of Persistent Antigenic Stimulation Modulates Adaptive Tolerance in Peripheral CD4+ T Cells. *The Journal of Experimental Medicine.* 2003;198(7):1107-1117.

44. Nagata Y, Kontani K, Enami T, et al. Variegated RHOA mutations in adult T-cell leukemia/lymphoma. *Blood.* 2016;127(5):596-604.

45. Ishikawa S. Opposite RHOA functions within the ATLL category. *Blood.* 2016;127(5):524-525.

46. Kiel MJ, Sahasrabuddhe AA, Rolland DCM, et al. Genomic analyses reveal recurrent mutations in epigenetic modifiers and the JAK-STAT pathway in Sezary syndrome. *Nat Commun.* 2015;6:8470.

47. Koskela HL, Eldfors S, Ellonen P, et al. Somatic STAT3 mutations in large granular lymphocytic leukemia. *N Engl J Med.* 2012;366(20):1905-1913.

48. Jerez A, Clemente MJ, Makishima H, et al. STAT3 mutations unify the pathogenesis of chronic lymphoproliferative disorders of NK cells and T-cell large granular lymphocyte leukemia. *Blood.* 2012;120(15):3048-3057.

49. Koo GC, Tan SY, Tang T, et al. Janus kinase 3-activating mutations identified in natural killer/T-cell lymphoma. *Cancer Discov.* 2012;2(7):591-597.

50. Kiel MJ, Velusamy T, Rolland D, et al. Integrated genomic sequencing reveals mutational landscape of T-cell prolymphocytic leukemia. *Blood.* 2014;124(9):1460-1472.

51. Bellanger D, Jacquemin V, Chopin M, et al. Recurrent JAK1 and JAK3 somatic mutations in T-cell prolymphocytic leukemia. *Leukemia.* 2014;28(2):417-419.

52. Nicolae A, Xi L, Pittaluga S, et al. Frequent STAT5B mutations in gammadelta hepatosplenic T-cell lymphomas. *Leukemia.* 2014;28(11):2244-2248.

53. Kucuk C, Jiang B, Hu X, et al. Activating mutations of STAT5B and STAT3 in lymphomas derived from gammadelta-T or NK cells. *Nat Commun.* 2015;6:6025.

54. Avbelj M, Wolz O-O, Fekonja O, et al. Activation of lymphoma-associated MyD88 mutations via allostery-induced TIR-domain oligomerization. *Blood.* 2014;124(26):3896-3904.

55. Wang C, McKeithan TW, Gong Q, et al. IDH2R172 mutations define a unique subgroup of patients with angioimmunoblastic T-cell lymphoma. *Blood.* 2015;126(15):1741-1752.

56. Sakata-Yanagimoto M. Multistep tumorigenesis in peripheral T cell lymphoma. *International Journal of Hematology.* 2015;102(5):523-527.

57. Quivoron C, Couronne L, Della Valle V, et al. TET2 inactivation results in pleiotropic hematopoietic abnormalities in mouse and is a recurrent event during human lymphomagenesis. *Cancer Cell.* 2011;20(1):25-38.

58. Cheminant M, Bruneau J, Kosmider O, et al. Efficacy of 5-Azacytidine in a TET2 mutated angioimmunoblastic T cell lymphoma. *Br J Haematol.* 2015;168(6):913-916.

Tables Legends

Table 1. Characteristics of the 70 variants identified by Targeted Deep Sequencing of TCR, JAK/STAT and TLR-related genes in 85 TFH-derived PTCL samples. Genes are organized by functional groups.

Figures Legends

Figure 1. Mutational landscape of nodal TFH-derived lymphomas. The results of targeted deep sequencing of 69 genes in 72 AITL (light grey) and 13 TFH-like PTCL (dark grey) are presented. Ten cases (8 AITL and 2 TFH-like PTCL) with no mutations detected are not represented. *TET2, DNMT3A* and *IDH2* mutations available for a subset of the cases reported in previous studies [8,9] are also shown. Case-mutation pairs for which data are not available are indicated by a 0. Mutated genes (rows) are arranged by decreasing order of mutation frequency. Patients (columns) are arranged from left to right based on their mutational status following gene ranking.

Figure 2. Mutations of TCR signaling-related genes in nodal lymphomas of TFH origin.

The intracellular pathways following TCR ligation and costimulatory activation were reconstructed using the Ingenuity pathway analysis (IPA) tools, the KEGG database and other references. Four main pathways are individualized, from left to right: (1) PI3K pathway following CD28/TCR-dependent FYN phosphorylation and ultimately resulting in CTNNB1

translocation into the nucleus; (2) NF-kB/NFAT pathway proximally initiated by ITK-dependent PLCG1 activation and resulting in NFAT1, NF-kB and IRF4 activation; (3) AP-1/MAPK pathway that comprises ITK-dependent GTF2I activation, MALT1-induced JNKs activation and PLCG1- GRB2/SOS-induced MAPK components activation; and (4) GTPase-dependent pathway, including RHOA, responsible for cytoskeleton remodelling upon co-stimulatory/TCR activation. The main positive interactions are indicated by solid green arrows, while inhibitory effects are indicated in red. The TCR signaling elements are depicted in yellow or red if the coding genes were mutated in <5% or 5% or more cases, respectively. The most frequently mutated genes (*PLCG1*, *CD*28, *PI3K* components, *CTNNB1* and *GTF2I*) were part of costimulatory, NF-kB/NFAT, PI3K and AP-1/MAPK intracellular signaling pathways. Proteins corresponding to wild type genes are indicated in blue, while genes that were not sequenced are in grey. ERK1, ERK2, JNK1, JNK2 and PDK1 are protein names for *MAPK1, MAPK3, MAPK8, MAPK9* and *PDPK1* genes respectively.

Figure 3. RHOA mutations in AITL and TFH-like PTCL. (A) Overview of the RHOA protein structure, showing G17V (42 AITL, 6 TFH-like PTCL) and the novel K18N (3 AITL) variants which target the highly conserved GTP/GDP binding site of RHOA. **(B)** Protein blot analysis of GTP-bound RHOA-Myc in rhotekin pulldown assay from HEK293T cells expressing indicated RHOA constructs. IP: immunoprecipitation. Representative of six independent experiments. **(C)** SRE (Serum Responsive Element) luciferase reporter assay monitoring the activity of RHOA K18N mutant, compared with WT, G14V or G17V mutants, previously characterized as activating and dominant negative respectively. Cells were stimulated (light grey) or not (dark grey) with FBS during 6 hours. Data are represented as mean ± sem (standard error

on mean) from four independent experiments. Significant differences in activation activity were determend using two-way ANOVA with repeated measurement (**, $p \leq 0.01$; ***, $p \leq 0.001$ compared to WT). **(D)** Representative western blot from a luciferase assay experiment. Ectopic myc tagged RHOA expression is revealed by anti-Myc. Anti-Actin blotting serves as loading control.

Figure 4. Mapping of variants in TCR signalling genes mutated in at least 3 patients. (A) CD28: the D124V/E variants involve the extracellular part of the receptor, while T195P lies in the intracellular, C-terminal domain, between the two domains allowing interaction with PIK3R1 (YVKM sequencce) or GRB2/VAV (PRRP sequence) proteins **(B**) FYN: the five mutations indicated occurred in three patients; one patient harboured two mutations (a); two mutations in adjacent positions in the SH3 domain (b) were observed on the same allele in another patient. (**C-E**) PI3K subunits: when appropriate cellular stimuli are present, the nSH2 and cSH2 domains of PIK3R1 bind phosphorylated tyrosines (YXXM motif) in activated receptors (CD28) and adapter proteins, thereby activating the PIK3CA (p110a) catalytic subunit without releasing the PIK3R1 (p85a) interaction with p110a through their iSH2 and ABD domains respectively. The K141R missense affects the Rho-GAP domain, while iSH2 and the second SH2 domains of PIK3R1 bore two missenses each (Q475P, T576A and G680S, V704M respectively). The A259V mutation, described as somatic in COSMIC, affects a linker region of PIK3R5. Finally, the L1001P point mutation affects the PIK3CA kinase domain. (**F**) PDK1: one inframe INDEL, one frameshift INDEL and three missense affect PDK1 protein. (**G**) CTNNB1: three previously described activating missenses affect the GSK3β inhibitory domain (exon 3), while the K335T activating mutation affects the armadillo repeats region (**H**) KRAS: three missense mutations

alter two N-terminal nucleotide binding regions. (**I**) GTF2I: five missense mutations affect the GTF2I transcription factor, among which two are found in different GTF2I-like domains. (**J**) VAV1: two frameshift deletion and two missenses affect VAV1, three being localized in the C-terminal SH3 domain of the protein. In all figure panels, previously described activating mutations are in green boldface, while mutations previously described but not functionally tested are underlined. PDK1 is the protein name of *PDPK1* gene.

Figure 5. Mapping and functional analysis of PLCG1 variants and CARD11 variants. (A) **S**chematic representation of PLCG1 protein with mapping of the 10 missense mutations identified in AITL (circles) or TFH-like PTCL (squares) cases. Previously described activating mutations are in green boldface and mutations previously described but not functionally tested are underlined. **(B)** Monitoring of PLCG1-mediated MALT1 activation via a FRET-based reporter assay. Data are represented as mean ± sem (standard error on mean) from three independent experiments. Significant differences in activation activity were determined using one-way ANOVA (**, $p \leq 0.01$; ***, $p \leq 0.001$). Representative western blot from a MALT1 activation experiment. PLCG1 expression is revealed by anti-Myc tag blotting while MALT1 expression is shown by anti-MALT1 antibody. **(C)** NFAT luciferase reporter assay monitoring activity of PLCG1 mutants, compared with previously-reported activating mutants (green). Data are represented as mean ± sem (standard error on mean). from seven independent experiments. Significant differences in activation activity were determend using one-way ANOVA (*, $p \leq 0.05$; **, $p \leq 0.01$). Representative western blot from a luciferase assay experiment. Ectopic myc tagged PLCG1 expression is revealed by anti-Myc. Anti-Actin blotting serves as loading control. **(D)** Schematic representation of CARD11 protein with mapping of the three point mutations found in

two AITL (circles) and one TFH-like PTCL-NOS (square) patients. A previously-described mutation is underlined. **(E)** Monitoring of CARD11-mediated MALT1 activation via a FRET-based reporter assay. Data are represented as mean ± sem (standard error on mean) from six independent experiments. Significant differences in activation activity were determined using one-way ANOVA (*, $p \leq 0.05$; **, $p \leq 0.01$). The known activating L244P variant (green) was used as a positive control for the experiment. Representative western blot from a MALT1 activation experiment. CARD11 expression is revealed by anti-HA tag blotting while MALT1 expression is shown by anti-MALT1 antibody. **(F)** NF-KB luciferase reporter assay in Jurkat cells deficient for *CARD11* monitoring activity of CARD11 mutants, compared with previously-reported activating mutants (green). Data are represented as mean ± sem from four independent experiments. Significant differences in activation activity were determined using two-way ANOVA (*, $p \leq 0.05$; **, $p \leq 0.01$; ***, $p \leq 0.001$ compared to WT PMA/IONO).

Figure 6. Mutual exclusivity of TCR signaling variants. The mutational status of TCR-related genes is represented for the 85 patients of the extended cohort. Genes other than *RHOA* are ranked by decreasing mutation frequency, and show an essentially mutually exclusive mutation pattern. In total, 49% of cases were mutated in one or several TCR-related gene(s) other than *RHOA* (hereafter considered as TCR_Mut), 28.5% were mutated in *RHOA* only and 22.5% harbored no mutation in any of the genes tested (collectively considered as TCR_WT).

Figure 7. Biological significance and clinical relevance of TCR signaling-related mutations **(A)** Spider plot representation of gene sets differentially enriched in patients with or without mutations in genes related to TCR signaling (TCR_Mut versus TCR_WT). Genes tested in the

enrichment analysis were selected from signatures relevant in T- and B-cell differentiation and activation. Statistical significance of the enrichment was reached for gene sets 1 to 15 ($p<0.05$); for gene set 16, marginal significance was observed ($p=0.1$). **(B, C)** Overall survival (OS, B) and progression-free survival (PFS, C) of patients with (red) or without (blue) mutations in TCR signaling-related genes. Analyses are restricted to the 59 patients treated with anthracyclin-based chemotherapy. Mutated patients show a trend toward a shorter PFS (11 vs 36 months) than WT patients ($p= 0.15$).

Functional Groups	GENE	Amino Acid Change	Mutation type	Domain	New/reported	Effect	References
co-stimulatory and proximal TCR signalling	*CD28*	D124V	missense	extracellular	AITL, ATLL	gain of function (F)	20, 25
	CD28	D124E	missense	extracellular	AITL, ATLL	gain of function (F)	20, 25
	CD28	T195P	missense	cytoplasmic	AITL, ATLL	gain of function (F)	20, 25, 31
	LCK	[b] N446K	missense	kinase	new	probably gain of function (P)	
	LCK	[b] P447R	missense	kinase	new	probably gain of function (P)	
	FYN	Q527X	stop gain		ATLL	probably gain of function (P)	20
	FYN	[a] 525_525del	frameshift deletion		new	probably gain of function (P)	
	FYN	[a] S186L	missense	SH2	new	probably gain of function (P)	
	FYN	[b] K108fs	frameshift deletion		new	probably loss of function (P)	
	FYN	[b] E107S	missense	SH3	new	probably loss of function (P)	
NF-kB/NF-AT pathway	*PLCG1*	E47K	missense	PH 1	ATLL	gain of function (F)	20
	PLCG1	R48W	missense	PH 1	ATLL, SS	no effect (F)	20, 24
	PLCG1	D342G	missense	PI-PLC X-box	ATLL, MF	gain of function (F)	20
	PLCG1	[a] S345F	missense	PI-PLC X-box	AITL, MF, SS, ATLL	gain of function (F)	20, 21, 22, 24
	PLCG1	[a] S520F	missense	PH 2; first part	MF, SS, ATLL	gain of function (F)	20, 21, 24
	PLCG1	E730K	missense	SH2 2	new	gain of function (F)	
	PLCG1	G869E	missense	near SH3	new	gain of function (F)	
	PLCG1	E1163K	missense	C2	ATLL, SS	gain of function (F)	20, 24
	PLCG1	D1165H	missense	C2	ATLL, SS	gain of function (F)	20, 24
	PLCG1	D1165G	missense	C2	ATLL	gain of function (F)	20
	CARD11	F902C	missense		ATLL	gain of function (F)	20
	CARD11	S547T	missense		new	gain of function (F)	
	CARD11	F176C	missense	coiled coil	new	gain of function (F)	
	TRAF6	Q347X	stop gain	coiled coil /MATH	new	NA	
PI3K pathway	*PIK3R1*	K141R	missense	RHO-GAP	new	probably gain of function (P)	
	PIK3R1	Q475P	missense	iSH2	new	probably gain of function (P)	
	PIK3R1	T576A	missense	iSH2	new	probably gain of function (P)	
	PIK3R1	G680S	missense	SH2 2	new	probably gain of function (P)	
	PIK3R1	V704M	missense	SH2 2	new	probably gain of function (P)	
	PIK3R5	A259V	missense		carcinoma (liver)	probably gain of function (P)	34
	PIK3CA	L1001P	missense	PI3K/PI4K	new	probably gain of function (P)	
	PDPK1	19_20del	inframe deletion		new	NA	
	PDPK1	151_152del	frameshift deletion	protein kinase	new	probably loss of function (P)	
	PDPK1	R324Q	missense	protein kinase	new	probably gain of function (P)	
	PDPK1	P340Q	missense	protein kinase	new	probably gain of function (P)	
	AKT1	G294R	missense	protein kinase	new	probably gain of function (P)	
	CTNNB1	[a] T41A	missense	Phospho by GSK3b	hepatocellular carcinoma, acute lymphoblastic leukaemia, breast cancer, wilms tumor	gain of function (F)	36
	CTNNB1	H36P	missense		hepatocellular carcinoma, acute lymphoblastic leukaemia, breast cancer, wilms tumor	gain of function (F)	36
	CTNNB1	[a] S45F	missense		hepatocellular carcinoma, acute lymphoblastic leukaemia, breast cancer, wilms tumor	gain of function (F)	36
	CTNNB1	K335T	missense		hepatocellular carcinoma	gain of function (F)	37
AP-1/MAPK pathway	*KRAS*	I36M	missense		haematopoeitic neoplasms	gain of function (F)	38
	KRAS	A18D	missense	GTP binding	lymphoma	gain of function (F)	38
	KRAS	G13D	missense	GTP binding	solid tumors	gain of function (F)	38
	MAPK3	R278Q	missense	protein kinase	new	probably gain of function (P)	
	STAT3	E616G	missense	SH2	lymphoma	gain of function (F)	26, 39
	STAT3	E616K	missense	SH2	lymphoma	gain of function (F)	26, 39
	GTF2I	D317E	missense		new	probably gain of function (P)	
	GTF2I	N340S	missense		new	probably gain of function (P)	
	GTF2I	R523S	missense	GTF2I-like	new	probably gain of function (P)	
	GTF2I	L607F	missense	GTF2I-like	new	probably gain of function (P)	
	GTF2I	R702Q	missense		new	probably gain of function (P)	
GTPases pathway	*RHOA*	K18N	missense	GTP binding	new	gain of function (F)	
	RHOA	G17V	missense	GTP binding	AITL, ATLL	dominant negative (F)	12, 13, 14, 20, 44
	VAV1	151_158del	frameshift deletion		new	probably loss of function (P)	
	VAV1	778_783del	frameshift deletion		new	NA	
	VAV1	D797G	missense	SH3 2	new	probably gain of function (P)	
	VAV1	Y826S	missense	SH3 2	new	probably gain of function (P)	
	VAV2	Y214C	missense	DH	gastric carcinoma	probably dominant negative (P)	
JAK/STAT and TLR pathways	*JAK1*	D831E	missense	kinase	new	probably gain of function (P)	
	JAK2	V617F	missense		myeloproliferative disorders	gain of function (F)	47-53
	JAK3	A699V	missense	kinase	lymphoma, carcinoma	gain of function (F)	47-53
	MYD88	S219C	missense	TIR	DLBCL, lymphocytic leukaemia	probably gain of function (P)	54

[a] gene variants found in the same patient but in different alleles

[b] gene variants found in the same patient and in the same allele

F: Functional validation; P: literature and models based

AITL: angioimmunoblastic T-cell lymphoma, ATLL: adult T-cell lymphoma/leukemia, SS: Sezary syndrome, MF: Mycosis Fungoides, DLBCL: diffuse large B-cell lymphoma

Table 1. Characteristics of the 70 variants identified by Targeted Deep Sequencing of TCR, JAK/STAT and TLR-related genes in 85 TFH-derived PTCL samples. Genes are organized by functional groups.

Figure 1

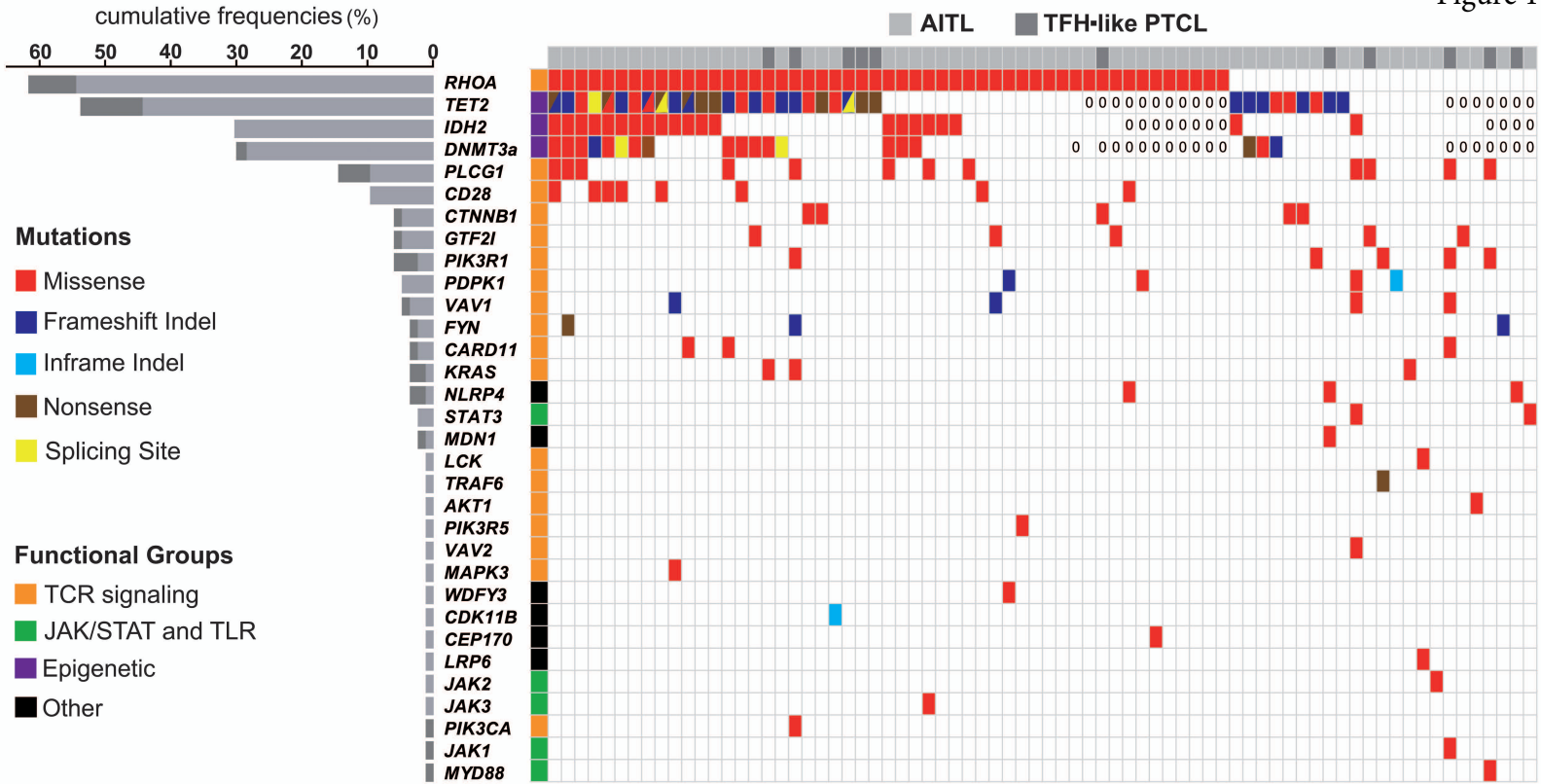
cumulative frequencies (%)
60
50
40
30
20
10
0
AITL
TFH-like PTCL
RHOA
TET2
IDH2
DNMT3a
PLCG1
CD28
CTNNB1
GTF2I
PIK3R1
PDPK1
VAV1
FYN
CARD11
KRAS
NLRP4
STAT3
MDN1
LCK
TRAF6
AKT1
PIK3R5
VAV2
MAPK3
WDFY3
CDK11B
CEP170
LRP6
JAK2
JAK3
PIK3CA
JAK1
MYD88
Mutations
Missense
Frameshift Indel
Inframe Indel
Nonsense
Splicing Site
Functional Groups
TCR signaling
JAK/STAT and TLR
Epigenetic
Other

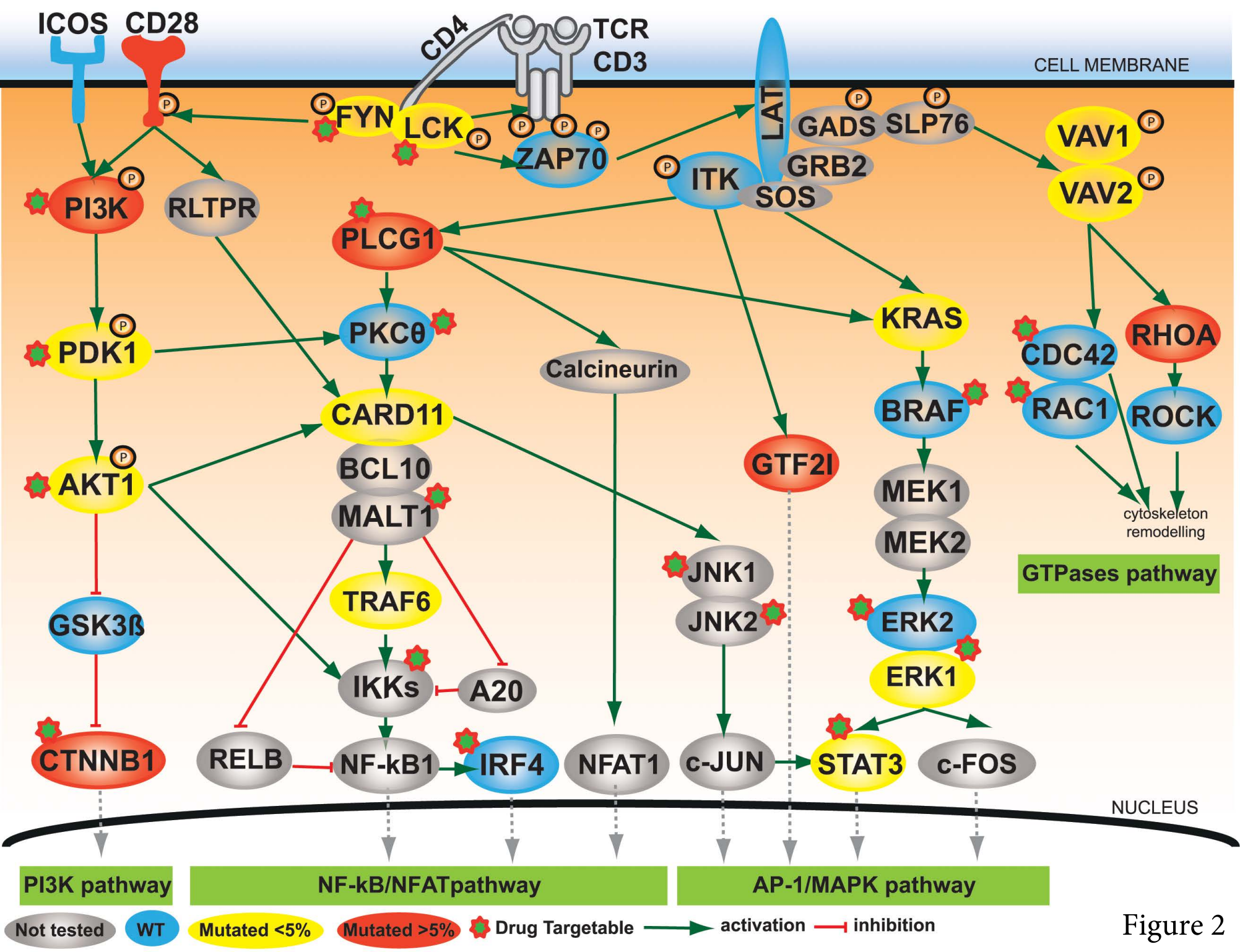
ICOS
CD28
CD4
TCR
CD3
CELL MEMBRANE
FYN
LCK
ZAP70
LAT
GADS
SLP76
ITK
GRB2
SOS
VAV1
VAV2
PI3K
RLTPR
PLCG1
PDK1
PKCθ
Calcineurin
KRAS
CDC42
RHOA
RAC1
ROCK
BRAF
CARD11
BCL10
MALT1
GTF2I
MEK1
MEK2
AKT1
cytoskeleton
remodelling
GTPases pathway
JNK1
JNK2
TRAF6
ERK2
ERK1
GSK3ß
IKKs
A20
CTNNB1
RELB
NF-kB1
IRF4
NFAT1
c-JUN
STAT3
c-FOS
NUCLEUS
PI3K pathway
NF-kB/NFATpathway
AP-1/MAPK pathway
Not tested
WT
Mutated <5%
Mutated >5%
Drug Targetable
activation
inhibition

Figure 2

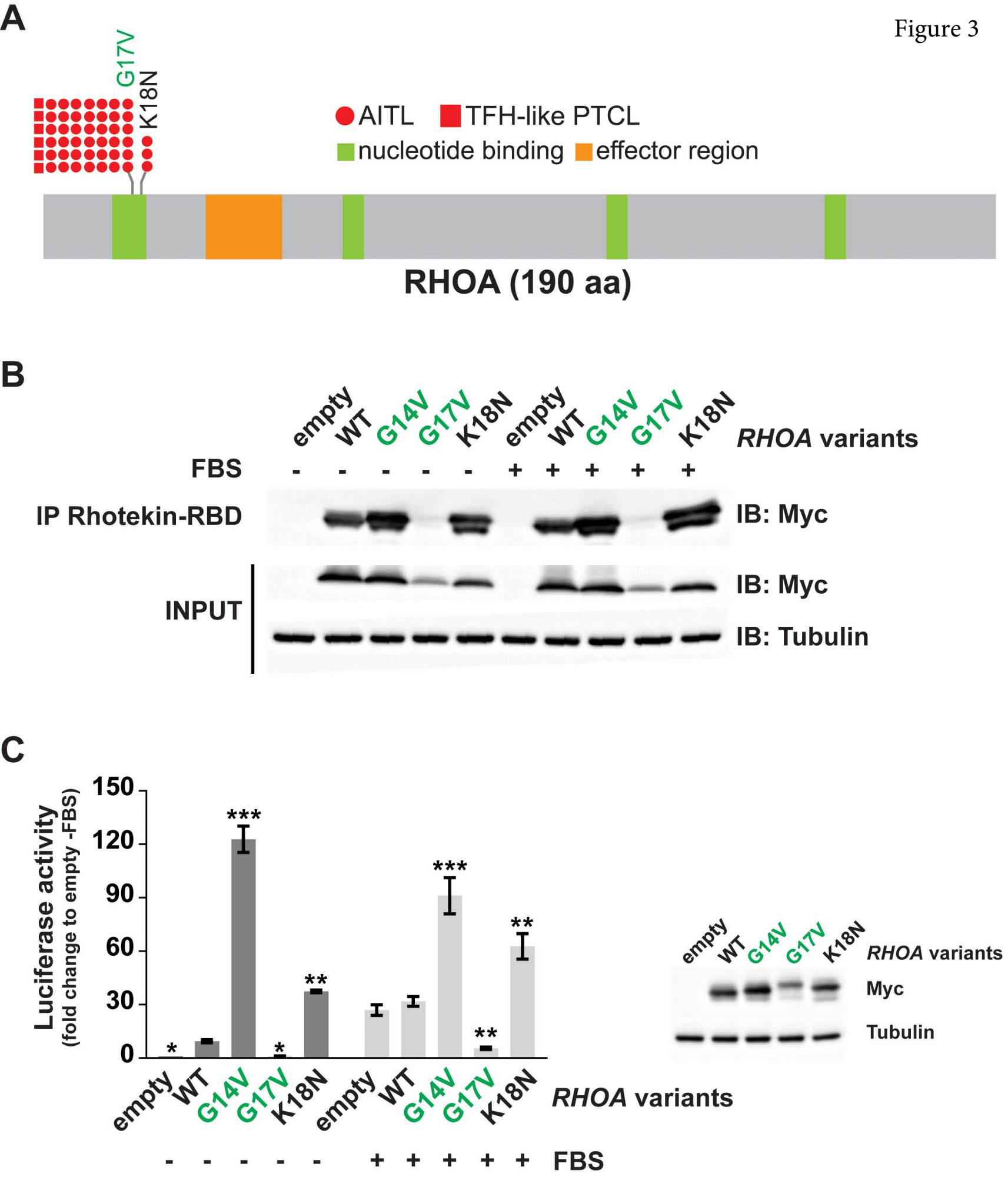
A
G17V
K18N
AITL
TFH-like PTCL
nucleotide binding
effector region
RHOA (190 aa)
B
empty
WT
G14V
G17V
K18N
RHOA variants
FBS
IP Rhotekin-RBD
IB: Myc
INPUT
IB: Myc
IB: Tubulin
C
Luciferase activity
(fold change to empty -FBS)
150
120
90
60
30
0
RHOA variants
FBS
Myc
Tubulin

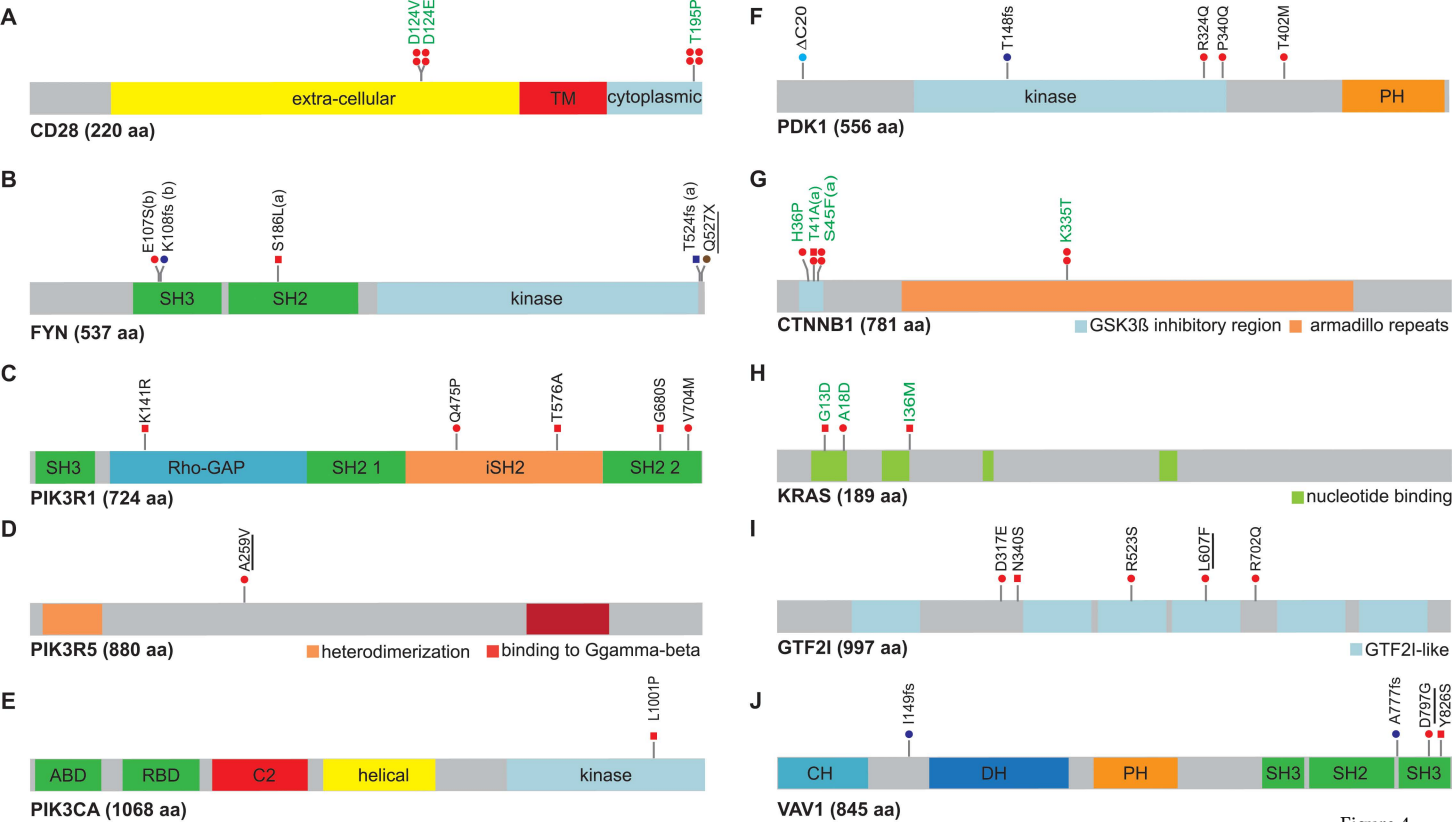
A
D124V
D124E
T195P
extra-cellular
TM
cytoplasmic
CD28 (220 aa)
B
E107S(b)
K108fs (b)
S186L(a)
T524fs (a)
Q527X
SH3
SH2
kinase
FYN (537 aa)
C
K141R
Q475P
T576A
G680S
V704M
SH3
Rho-GAP
SH2 1
iSH2
SH2 2
PIK3R1 (724 aa)
D
A259V
PIK3R5 (880 aa)
heterodimerization
binding to Ggamma-beta
E
L1001P
ABD
RBD
C2
helical
kinase
PIK3CA (1068 aa)
F
ΔC20
T148fs
R324Q
P340Q
T402M
kinase
PH
PDK1 (556 aa)
G
H36P
T41A(a)
S45F(a)
K335T
CTNNB1 (781 aa)
GSK3ß inhibitory region
armadillo repeats
H
G13D
A18D
I36M
KRAS (189 aa)
nucleotide binding
I
D317E
N340S
R523S
L607F
R702Q
GTF2I (997 aa)
GTF2I-like
J
I149fs
A777fs
D797G
Y826S
CH
DH
PH
SH3
SH2
SH3
VAV1 (845 aa)
AITL
TFH-like PTCL
missense
inframe indel
frameshift indel
stop gain

Figure 4

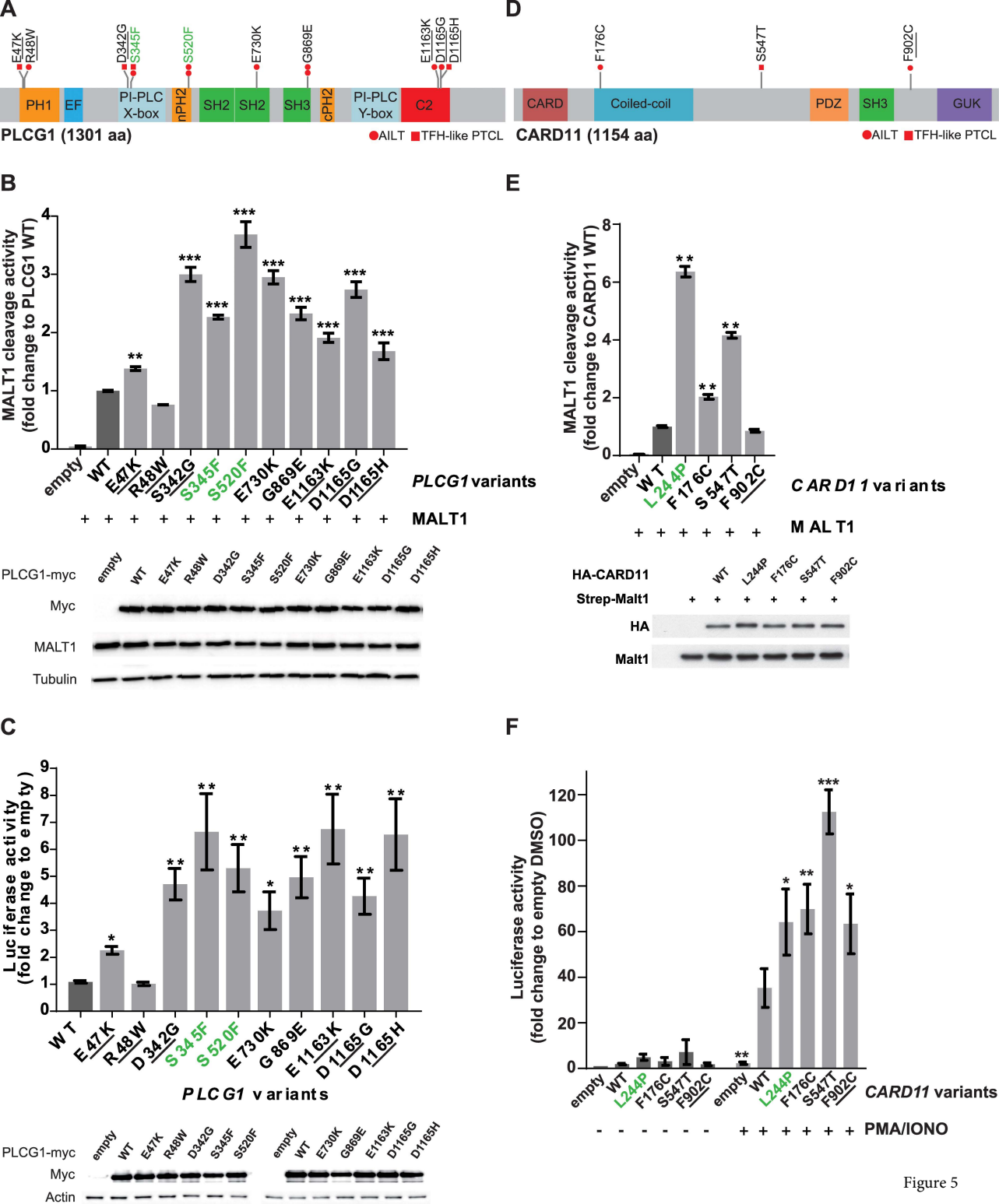
A
E47K
R48W
D342G
S345F
S520F
E730K
G869E
E1163K
D1165G
D1165H
PH1
EF
PI-PLC X-box
nPH2
SH2
SH2
SH3
cPH2
PI-PLC Y-box
C2
PLCG1 (1301 aa)
AILT
TFH-like PTCL
D
F176C
S547T
F902C
CARD
Coiled-coil
PDZ
SH3
GUK
CARD11 (1154 aa)
AILT
TFH-like PTCL
B
MALT1 cleavage activity (fold change to PLCG1 WT)
empty
WT
E47K
R48W
S342G
S345F
S520F
E730K
G869E
E1163K
D1165G
D1165H
PLCG1 variants
MALT1
PLCG1-myc
Myc
MALT1
Tubulin
E
MALT1 cleavage activity (fold change to CARD11 WT)
empty
WT
L244P
F176C
S547T
F902C
CARD11 variants
MALT1
HA-CARD11
Strep-Malt1
HA
Malt1
C
Luciferase activity (fold change to empty)
WT
E47K
R48W
D342G
S345F
S520F
E730K
G869E
E1163K
D1165G
D1165H
PLCG1 variants
PLCG1-myc
Myc
Actin
F
Luciferase activity (fold change to empty DMSO)
empty
WT
L244P
F176C
S547T
F902C
CARD11 variants
PMA/IONO

Figure 5

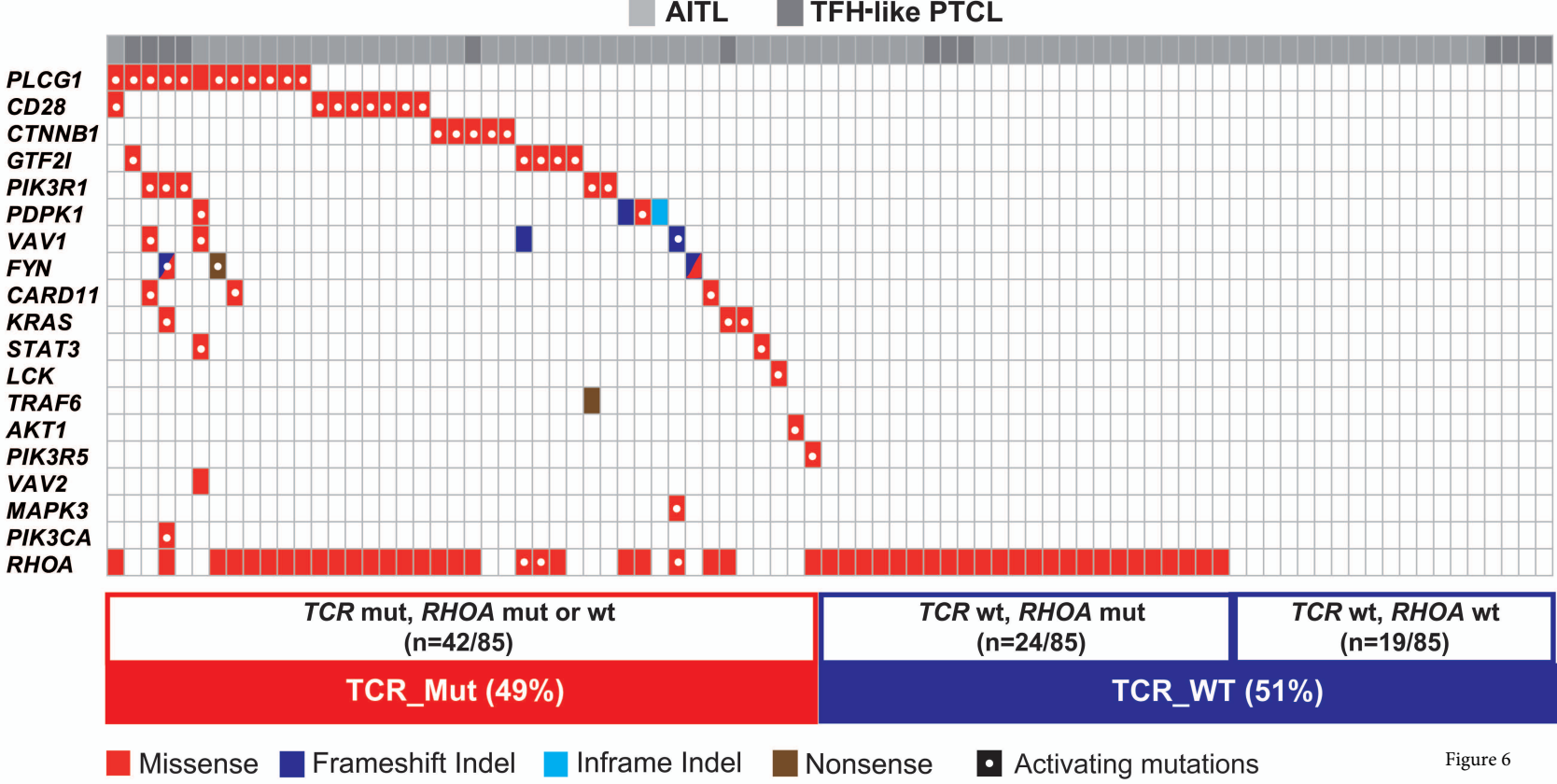
AITL
TFH-like PTCL
PLCG1
CD28
CTNNB1
GTF2I
PIK3R1
PDPK1
VAV1
FYN
CARD11
KRAS
STAT3
LCK
TRAF6
AKT1
PIK3R5
VAV2
MAPK3
PIK3CA
RHOA
TCR mut, RHOA mut or wt
(n=42/85)
TCR wt, RHOA mut
(n=24/85)
TCR wt, RHOA wt
(n=19/85)
TCR_Mut (49%)
TCR_WT (51%)
Missense
Frameshift Indel
Inframe Indel
Nonsense
Activating mutations

Figure 6

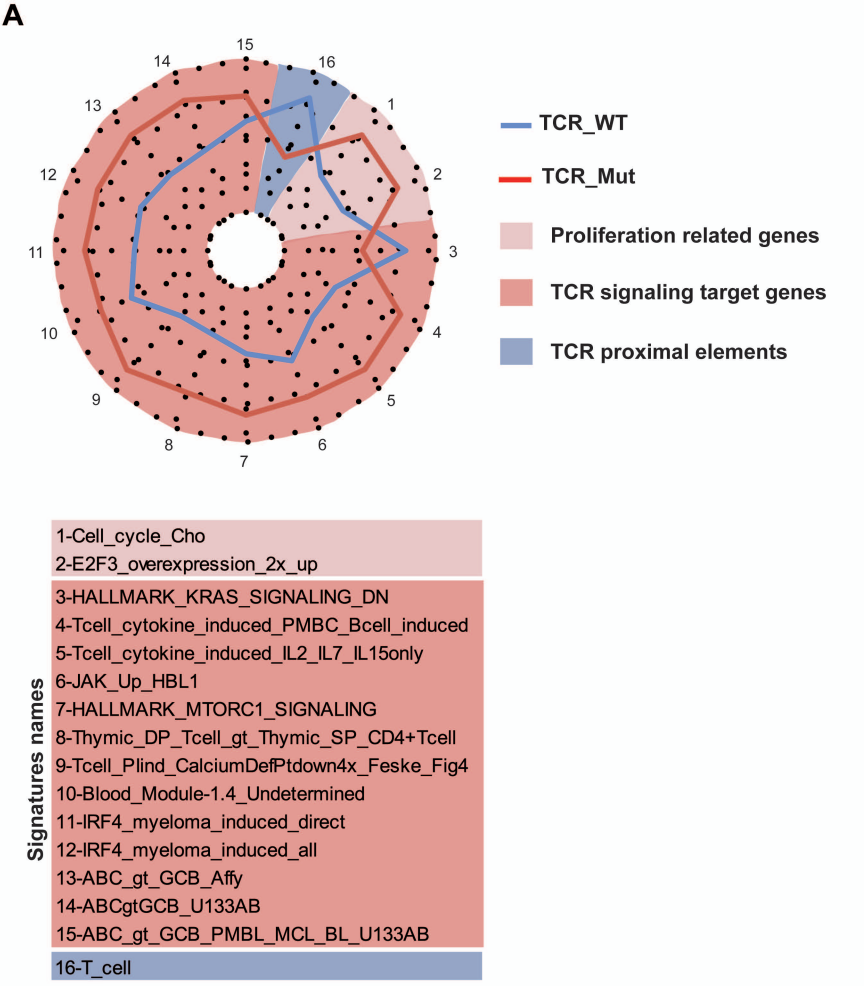
A
15
14
16
13
1
12
2
11
3
10
4
9
5
8
6
7
TCR_WT
TCR_Mut
Proliferation related genes
TCR signaling target genes
TCR proximal elements
Signatures names
1-Cell_cycle_Cho
2-E2F3_overexpression_2x_up
3-HALLMARK_KRAS_SIGNALING_DN
4-Tcell_cytokine_induced_PMBC_Bcell_induced
5-Tcell_cytokine_induced_IL2_IL7_IL15only
6-JAK_Up_HBL1
7-HALLMARK_MTORC1_SIGNALING
8-Thymic_DP_Tcell_gt_Thymic_SP_CD4+Tcell
9-Tcell_Plind_CalciumDefPtdown4x_Feske_Fig4
10-Blood_Module-1.4_Undetermined
11-IRF4_myeloma_induced_direct
12-IRF4_myeloma_induced_all
13-ABC_gt_GCB_Affy
14-ABCgtGCB_U133AB
15-ABC_gt_GCB_PMBL_MCL_BL_U133AB
16-T_cell

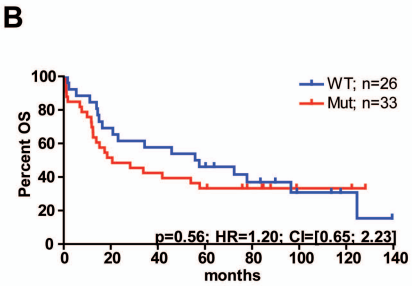
B
Percent OS
100
80
60
40
20
0
WT; n=26
Mut; n=33
p=0.56; HR=1.20; CI=[0.65; 2.23]
0
20
40
60
80
100
120
140
months

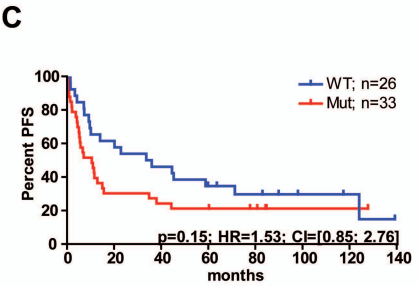
C
Percent PFS
100
80
60
40
20
0
WT; n=26
Mut; n=33
p=0.15; HR=1.53; CI=[0.85; 2.76]
0
20
40
60
80
100
120
140
months

Prepublished online July 1, 2016;
doi:10.1182/blood-2016-02-698977

Activating mutations in genes related to TCR signaling in angioimmunoblastic and other follicular helper T-cell-derived lymphomas

David Vallois, Maria Pamela D. Dobay, Ryan D. Morin, François Lemonnier, Edoardo Missiaglia, Mélanie Juilland, Justyna Iwaszkiewicz, Virginie Fataccioli, Bettina Bisig, Annalisa Roberti, Jasleen Grewal, Julie Bruneau, Bettina Fabiani, Antoine Martin, Christophe Bonnet, Olivier Michielin, Jean-Philippe Jais, Martin Figeac, Olivier A. Bernard, Mauro Delorenzi, Corinne Haioun, Olivier Tournilhac, Margot Thome, Randy D. Gascoyne, Philippe Gaulard and Laurence de Leval

Blood (print ISSN 0006-4971, online ISSN 1528-0020), is published weekly by the American Society of Hematology, 2021 L St, NW, Suite 900, Washington DC 20036.

Appendix

Participants of the Tenomic consortium:

A. Martin, Hôpital Avicenne, Bobigny, France; I. Soubeyran, P. Soubeyran, Institut Bergonié, Bordeaux, France; P. Dechelotte, A. Pilon, O.Tournilhac, Hôtel-Dieu, Clermont-Ferrand, France; P. Gaulard, C. Copie-Bergman, M.H. Delfau, J. Moroch, F. Le Bras, J. Dupuis, C. Haioun, Hôpital H. Mondor, Créteil, France; T. Petrella, L. Martin, JN.. Bastié, O. Casasnovas CHU, Dijon, France; B. Fabre, R. Gressin, D. Leroux, MC Jacob CHU, Grenoble, France; L. de Leval, B. Bisig, E. Missiaglia, A. Cairoli, CHUV, Lausanne, Suisse; C. Bonnet, CHU Sart-Tilman, Liège, Belgique; M.C. Copin, B. Bouchindhomme, F. Morschhauser, CHU, Lille, France; B. Petit, A. Jaccard, Hôpital Dupuytren, Limoges, France; F. Berger, B. Coiffier, CHU Sud, Lyon, France; T. Rousset, P. Quittet, G. Cartron, Hôpital Gui de Chauliac-St Eloi, Montpellier, France; S. Thiebault, B. Drenou, Hôpital E. Muller, Mulhouse, France; K. Montagne, C. Bastien, S. Bologna, CHU de Brabois, Nancy, France; C. Bossard, S. Le Gouill, Hôtel-Dieu, Nantes, France; J. Brière, D. Sibon, C. Gisselbrecht, J. Soulier, Hôpital St Louis, Paris, France; B. Fabiani, A. Aline-Fardin, P. Coppo, Hôpital Saint-Antoine, Paris, France; F. Charlotte, J. Gabarre, Hôpital Pitié- Salpétrière, Paris, France; T. Molina, J. Bruneau, D. Canioni, V. Verkarre, E. Macintyre, V. Asnafi, O. Hermine, R. Delarue, JP Jaïs, Hôpital Necker, Paris, France; M. Parrens, J.P. Merlio, K. Bouabdallah, Hôpital Haut Lévêque, Bordeaux, France; S. Maugendre-Caulet, P. Tas, F. Llamas-Gutierrez T. Lamy, CHU Pontchaillou, Rennes, France; J.M. Picquenot, F. Jardin, C. Bastard, Centre H Becquerel, Rouen, France; M. Peoch', J. Cornillon, CHU, Saint Etienne, France; L. Lamant, C. Laurent, G. Laurent, L. Ysebaert, Hôpital Purpan, Toulouse, France; J.Bosq, P. Dartigues, V. Ribrag, Institut G Roussy, Villejuif, France; M. Patey, A. Delmer, Hôpital R. Debré, Reims, France; J.F. Emile, K. Jondeau,

Hôpital Ambroise Paré, Boulogne, France; M.C. Rousselet, M. Hunault, CHU, Angers, France ; C. Badoual, Hôpital Européen Georges Pompidou, Paris; C. Legendre, S. Castaigne, A.L. Taksin, CH Versailles, Le Chesnay, France; J. Vadrot, B. Joly, A. Devidas, CH Sud Francilien, Corbeil, France; G. Damaj, CHU Caen, France; P. Dessen, G Meurice, Institut G. Roussy, Villejuif, France; M. Delorenzi, MP Dobay, Swiss Institut of Bioinformatics, Lausanne, Suisse; F Radvanyi, E. Chapeaublanc, Institut Curie, Paris, France; S. Spicuglia, CIML, Marseille, France; C. Thibault, IGBMC, Illkirsch, France; V. Fataccioli, project coordinator, Hôpital H. Mondor, Créteil, France.

Supplementary methods

RHOA Pull-down assay

$2x10^6$ HEK293T cells were lipofected 24 h after seeding in 10 cm dishes with 20 µg of indicated constructs. Twenty-four hours later, cells were serum-starved for another 24h period. Then, cells were harvested or serum-stimulated during 20 minutes. Serum-starved and serum-stimulated cells were washed once with ice-cold PBS and lysed in IP buffer (50 mM Tris, 10 mM $MgCl_2$, 0.3 M NaCl, 2% IGEPAL, 1mM PMSF, Protease Inhibitor Cocktail 1X (Roche) and Phosphatase Inhibitor Cocktail 1X (Roche)). After clearing of lysates by centrifugation, protein content was quantified using the Precision Red advanced Protein Assay (Cytoskeleton). Next, lysates containing 200 µg of protein were incubated with 40 µL of Rhotekin-RBD beads (Cytoskeleton) for one hour at 4°C with rotation. After incubation, beads were washed twice in ice-cold wash buffer (25 mM Tris, pH 7.5, 30 mM $MgCl_2$ and 40 mM NaCl) and resuspended with 30 µL of 2x Laemmli buffer. The presence of Myc-tagged activated RHOA associated with Rhotekin-RBD beads was determined by immunoblotting with an anti-Myc antibody (Millipore).

Luciferase-based activity assays

The analysis of the activity of *RHOA, PLCG1* and *CARD11* mutants was performed using SRE (Serum Responsive Element; Promega, Madison, WI, USA), NFAT (Addgene, Cambridge, MA, USA) and NF-kB (Promega, Madison, WI, USA) luciferase-based reporter systems, respectively.

For *RHOA and PLCG1:* 50'000 HEK293T cells/well were lipofected (Lipofectamin 2000, Lifetechnologies, Carlsbad, CA, USA) 24h after seeding with 10 ng of Renilla luciferase vector, 400 ng of the Firefly luciferase reporter and 300 ng of PLCG1 or RHOA constructs. Twenty-four hours later, Firefly and Renilla luciferase activities were measured using the Dual-Luciferase Reporter Assay System from Promega according to manufacturer's instructions (Promega, Madison, WI, USA).

For *CARD11*: $10x10^6$ Jurkat cells deficient for *CARD11*[29] (kindly provided by Dr. Xin Lin) were electroporated (BioRad, Hercules, California, USA) with 200 ng of Renilla luciferase vector, 5 µg of the NF-kB (Promega, Madison, WI, USA) Firefly luciferase reporter, 5 µg of a Large T expressing plasmid and 10 µg of CARD11 constructs. Fourty-eight hours later, Firefly and Renilla luciferase activities were measured using the Dual-Luciferase Reporter Assay System from Promega according to manufacturer's instructions (Promega, Madison, WI, USA).

FRET (Fluorescence Resonance Energy Transfer)-based MALT1 activity assays

FRET-based reporter assays were performed to assess CARD11 and PLCG1-dependent MALT1 protease activation in HEK293T cells as previously described[28]. 85'000 HEK293T cells were transfected with the eYFP–Leu-Val-Ser-Arg–eCFP reporter construct (which served as a MALT1 substrate), together with combinations of CARD11 or PLCG1 variants and MALT1 and BCL10 expression constructs. Twenty-four hours after transfection, cells were washed and resuspended in flow cytometry buffer (2% FCS in PBS) and analyzed with an LSR II flow

cytometer (BD Biosciences) containing 405-, 488-, 561- and 640-nm lasers. To measure the eCFP and FRET signals, the transfected cells were excited with a standard 450/50 filter for collection of the eCFP fluorescence and a 585/42 filter for FRET fluorescence, respectively, and for each sample at least 5'000 highly eYFP+ cells were counted. Significant differences in activation activity were determined using one-way ANOVA (**, $p \leq 0.01$; ***, $p \leq 0.001$) Analysis was performed using a Repeated measures one-way ANOVA test with Dunett correction for multiple comparisons.

Supplemental Figures

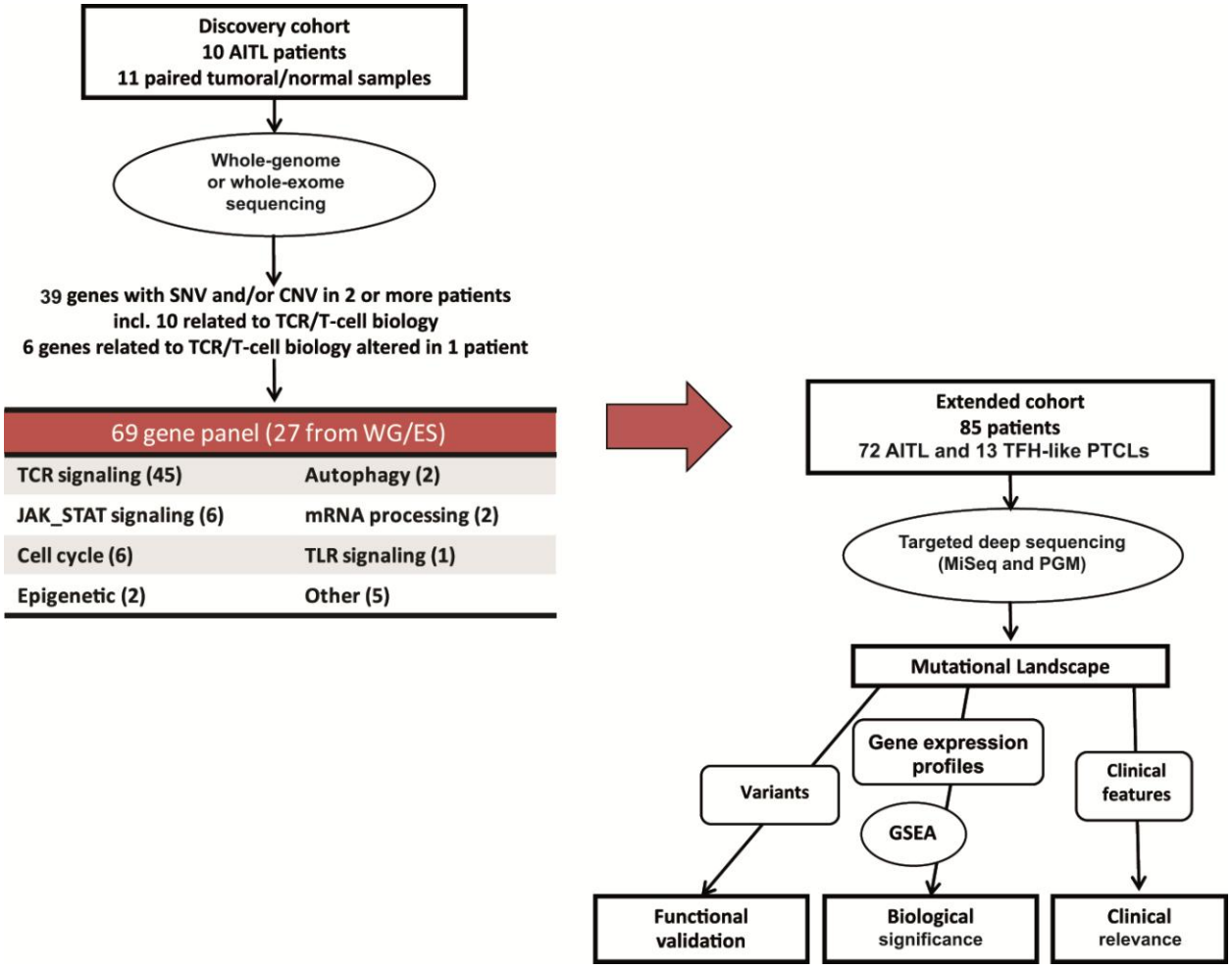

Figure S1: Study workflow.
WGS and WES of 11 paired normal and tumor samples from 10 AITL patients were used to screen for genes altered in at least two cases (SNV and/or CNV) or altered in one patient but relevant to TCR signaling or T-cell biology. A panel of 69 candidate genes, including 45 related to TCR and 7 related to T-cell biology signaling, were selected for deep sequencing in an extended cohort comprised of 72 AITL and 13 TFH-like PTCL-NOS tumor samples at diagnosis. Integrated analysis of the mutational status together with clinical information and gene expression profiles (GEP; 65 AITL and 12 TFH-like PTCL, NOS) was performed to assess the clinical and biological relevance of the detected variants.

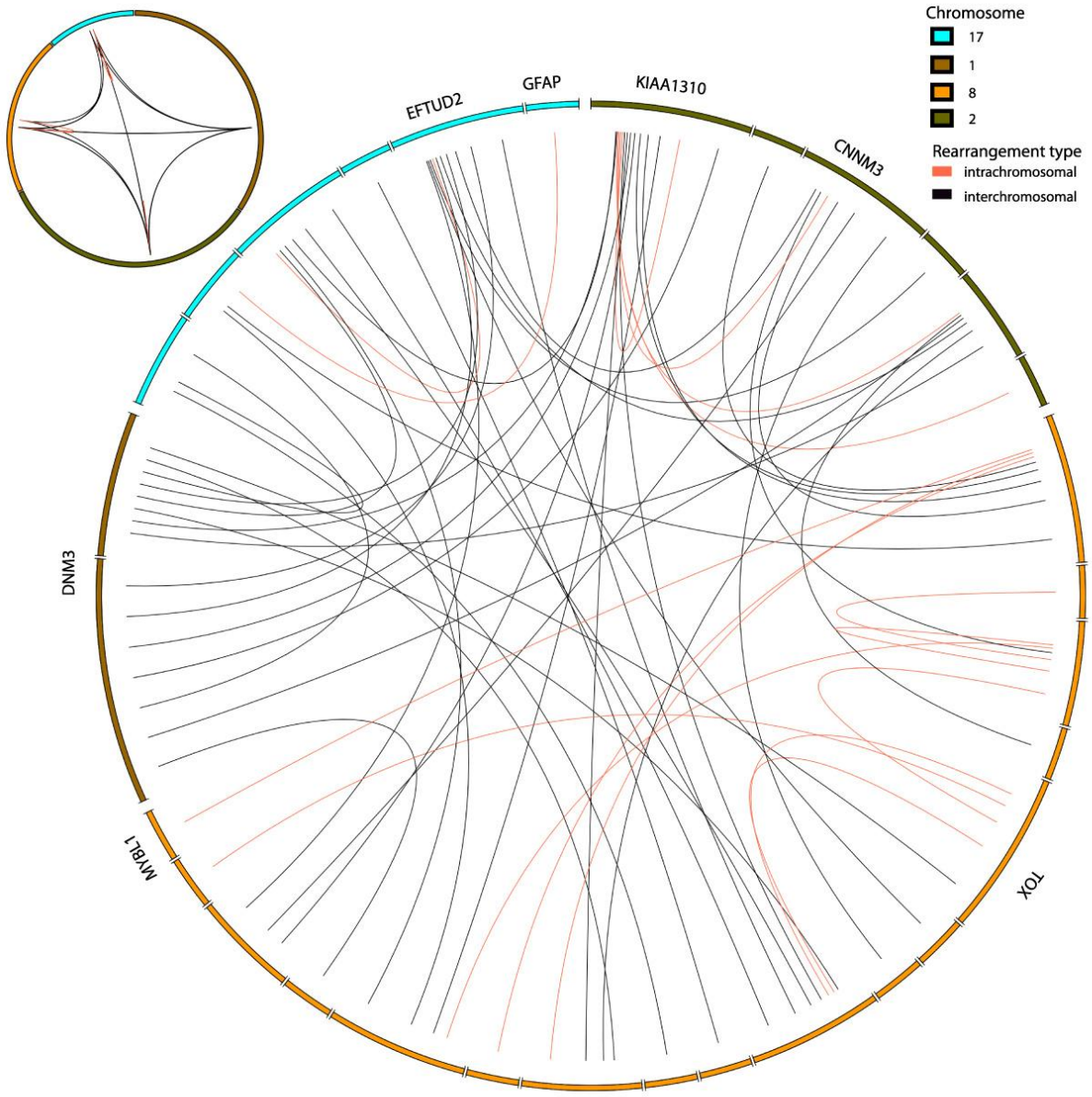

Figure S2: Chromosomal rearrangements from patient with chromotripsis pattern.
In one patient, a striking number of structural variation (SV) breakpoints and SNVs were detected in the tumor genome. 116 of these breakpoints could be attributed to an apparent chromothripsis event owing to linkages between these and a restricted set of loci in the genome. In the inset (upper left), the four affected chromosomes are shown with the individual intra- and interchromosomal rearrangements represented as arcs. Expansion of the regions containing breakpoints shows the full scope of SVs involved in this event. Of note, breaks affected introns or exons of a total of seven genes with the approximate coordinates of the genes indicated with gene symbols. The chromosome with the most SV breakpoints was 8, and many of these affected the TOX gene. This gene encodes a protein with a high mobility group (HMG) DNA binding domain thought to play a role in T-cell development. Structural alterations (including homozygous deletions) affecting TOX have recently been found to be common in primary central nervous system lymphomas.

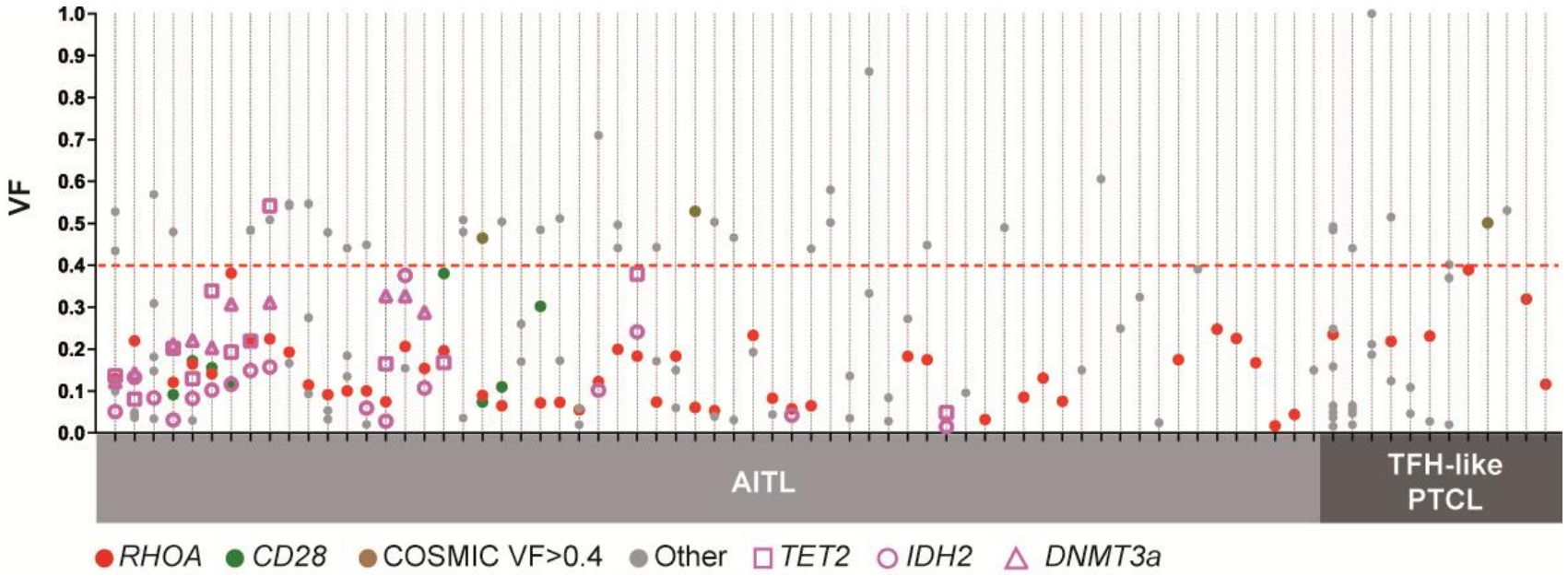

Figure S3: Variants frequencies distribution.
The 103 variants were found in 45 out of 69 deep-sequenced candidate genes in 85 AITL or TFH-like PTCL-NOS patients are represented. Variant frequencies (VF) were plotted for each patient. A VF threshold of 0.4 (red dotted line, chosen based on the maximum VF of *RHOA* and *CD28* variants) was used to discriminate potential somatic from germline variants. Variants with VF above 0.4 but previously described somatic and/or with functional relevance (CARD11) (brown dots) were not filtered out. A total of 70 variants were kept for further analysis. *TET2*, *DNMT3A* and *IDH2* results are from a previous study (19 patients sequenced on PGM platform are shown).

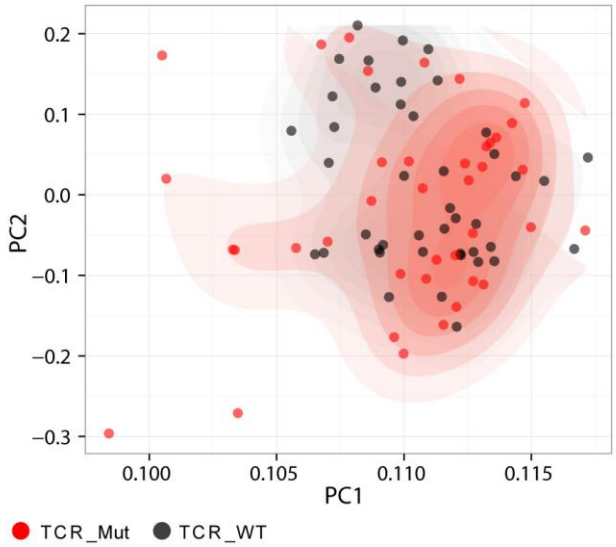

Figure S4: Principal component analysis (PCA) of AITLs and TFH-like PTCL-NOS coloured based on TCR pathway mutation status.
PCA of GEP from TCR_Mut and TCR_WT patients indicate that the main sources of variability in AITL and TFH-like PTCL-NOS groups are not principally linked to TCR status; heterogeneity within AITL and TFH-like PTCL-NOS thus masks differences in gene expression in TCR_Mut and TCR_WT.

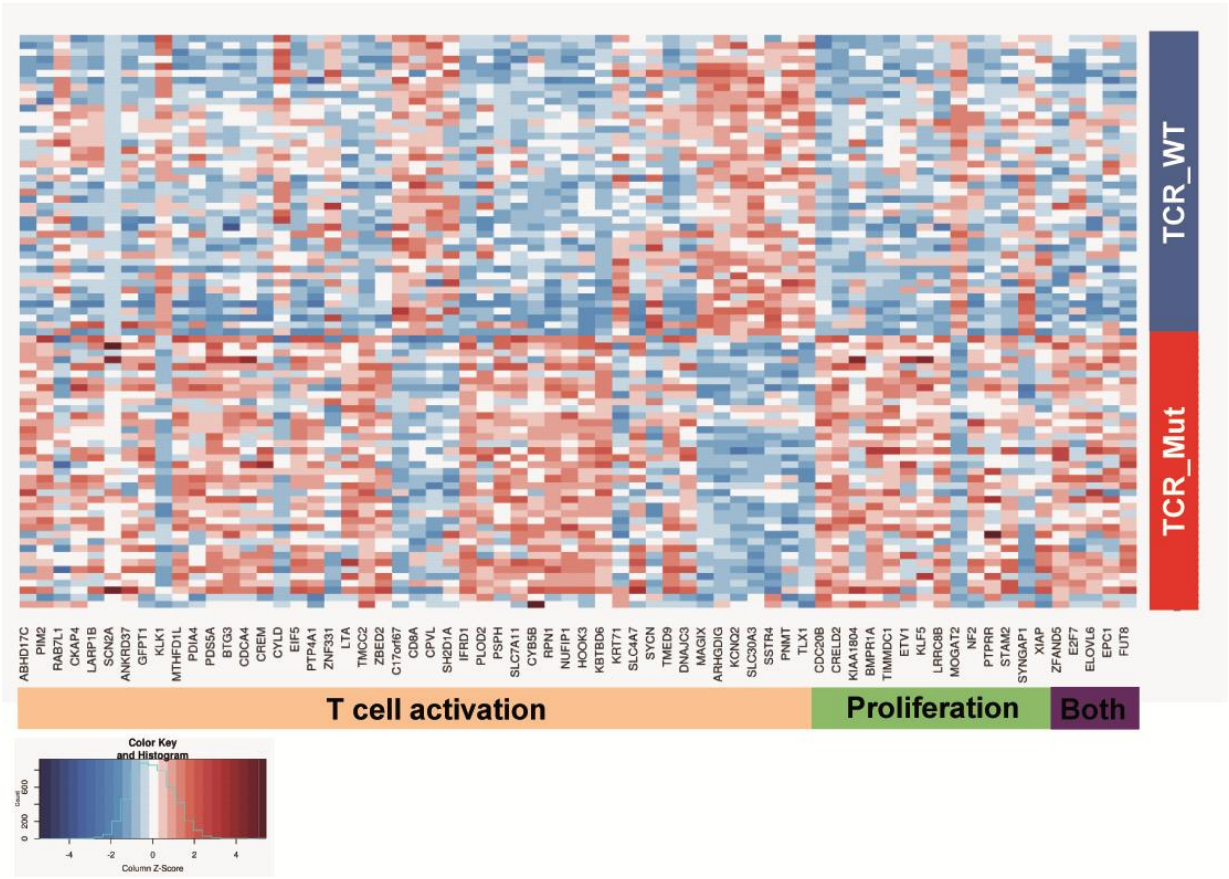

Figure S5: Heatmap of leading edge genes in patients with or without mutations in TCR pathways related genes.

Clustering was performed according to (i) the patients' mutational status in TCR related pathways (mutants, red and wt, blue) and (ii) hierarchy of expression profile of leading edge genes grouped into two categories (T-cell activation, proliferation or both gene signatures). Only leading edge genes from gene sets presented in Figure 4 are shown.

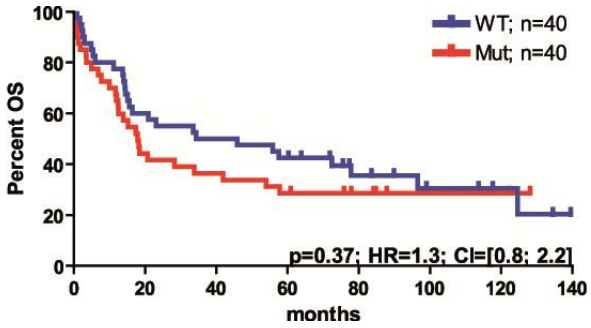

Figure S6: Overall survival (OS) of patients with (red) or without (blue) mutations in TCR signaling-related genes was compared using the Kaplan-Meier method.
Analysis was performed on all 80 patients with available clinical information. Mut: mutated; WT: wild type; Mo: months; p: p value; HR: Hazard Ratio; CI: Confidence Interval.

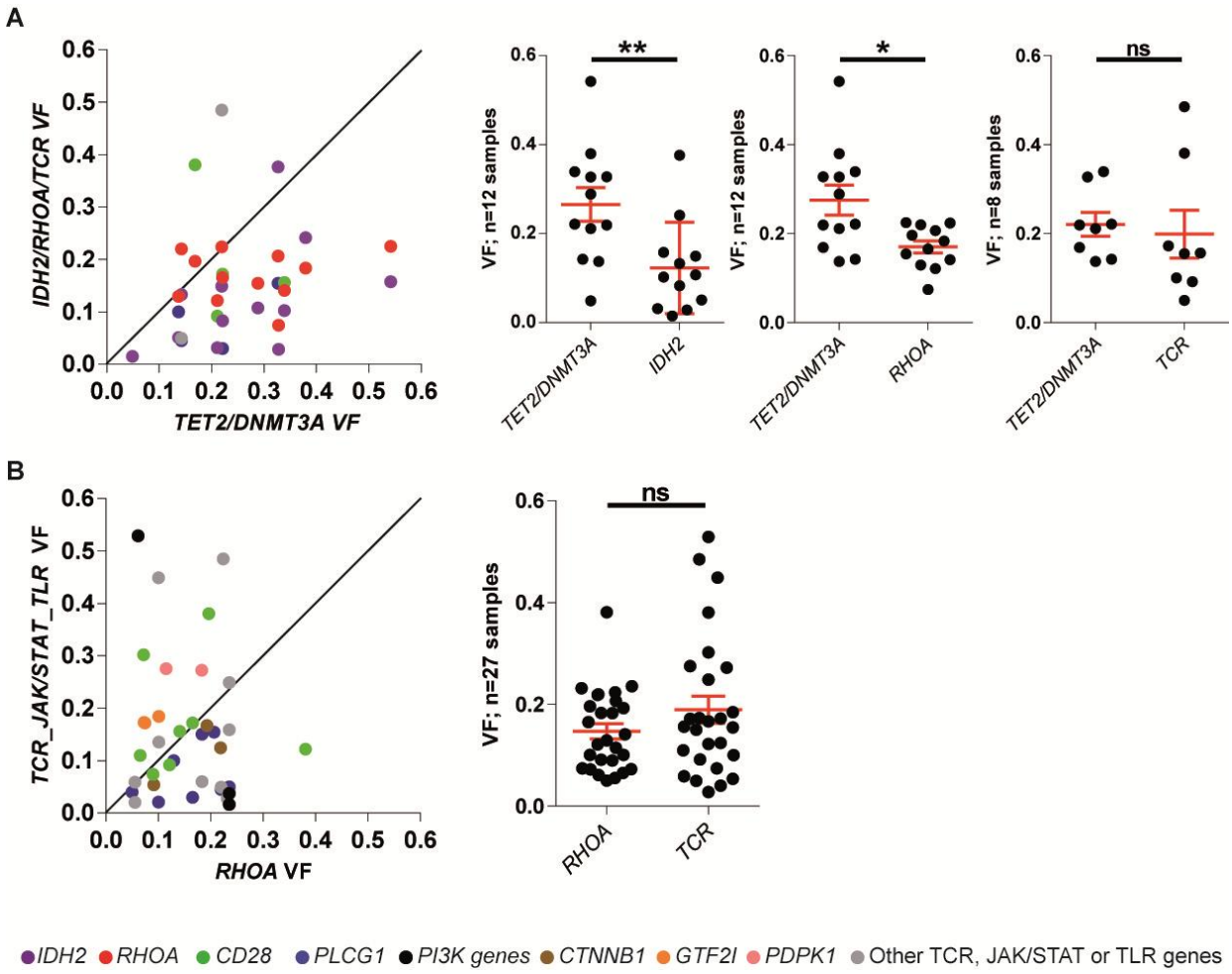

Figure S7: Analysis of allele frequencies of selected mutations in patients harboring mutations in multiple genes. (A) Comparison of Variant Frequencies of mutations in 13 samples harboring mutations in *TET2/DNMT3A* co-occuring with *RHOA*, *IDH2* or *TCR, JAK/STAT, TLR* signaling pathways. Mean VF of *TET2/DNMT3A* was compared to those of *IDH2*, *RHOA* or *TCR, JAK/STAT, TLR* signaling pathways. When mutations occurred in both *TET2* and *DNMT3A* or in the same genes, the highest VF was recorded. **(B)** Comparison of VFs of mutations in 27 samples harboring mutations in *RHOA* co-occuring with mutations in *co-stimulatory/TCR* signaling related, *JAK/STAT* or *TLR* signaling. When *co-stimulatory/TCR* related, *JAK/STAT* or *TLR* signaling mutations were co-occuring, the highest VF was taken into consideration. Spearman correlation coefficients were calculated for relevant data pairs. Mean VF were compared using a Wilcoxon matched-pairs signed rank test.

Sample	sequencing	age at diagnosis	stage	IPI	status (follow up in months)	Type of sample (months after diagnostic)	treatment received before biopsy	source of tumor DNA	source of germline DNA	TCR clonality in germline DNA
TENOM04.119	WGS	69	IV	5	dead (6)	relapse (5)	CHOP	blood (leukemic dissemination, FACS sorted)	saliva	negative
TENOM04.121	WGS	69	IV	3	alive (18)	diagnosis	none	lymph node (cell suspension, FACS sorted)	blood	ND
TENOM04.026	WGS	70	IV	4	alive (126)	diagnosis	none	lymph node (tissue)	blood	negative
TENOM04.060	WGS	71	IV	4	alive (70)	diagnosis	none	lymph node (tissue)	blood	ND
TENOM28.001	WGS	66	IV	4	dead (47)	diagnosis	none	lymph node (tissue)	blood	negative
TENOM07.025	WGS	48	IV	4	dead (13)	diagnosis	none	lymph node (tissue)	blood	ND
TENOM07.025	WGS	48	IV	4	dead (13)	refractory (2.5)	CHOP	lymph node (tissue)	blood	ND
TENOM04.120	WGS	58	III	1	alive (11)	relapse (9.5)	CHOP	lymph node (cell suspension, FACS sorted)	blood	negative
TENOM04.065	WES	52	IV	2	dead (105)	relapse (43)	COPADEM/CYVE/CHOP	lymph node (tissue)	blood	negative
TENOM04.081	WES	62	IV	3	dead (20.6)	diagnosis	none	lymph node (tissue)	blood	negative
TENOM04.115	WES	68	IV	5	dead (10.8)	relapse (4)	CHOP/DHAP	peritoneal effusion	blood	negative

Table S1. Description of the 10 AITL patients of the discovery cohort.

WGS: Whole Genome Sequencing
WES: Whole Exome Sequencing
CHOP: Cyclophosphamide Hydroxydonorubicin Oncovin Prednisone
COPADEM: Cyclophosphamide Oncovin Prednisone Adriamycine Methotrexate
CYVE: Cytarabine Etoposide
DHAP: Dexamethasone Cytarabine Cisplatin

	whole cohort	AITL	TFH-like PTCL	statistics	
				p value	test
N	85	72	13		
sex					
male	50	42	8	1	F
female	35	30	5		
median age (quartile)	65 (56-74)	65 (56-75)	62 (59-67)	0.4	MW
stage					
I	0	0	0	0.2	F
II	1	0	1		
III	21	17	4		
IV	56	49	7		
LDH					
>N	52	44	8	0.73	F
≤N	21	17	4		
hemoglobin					
<10 g/dL	21	19	2	0.48	F
≥10 g/dL	46	38	8		
platelets					
<100000	4	3	1	0.5	F
≥100000	60	51	9		
hypergammaglobulinemia					
yes	23	20	3	0.7	F
no	22	18	4		
Direct coombs test					
positive	28	27	1	1	F
negative	17	16	1		
ECOG					
0-1	39	30	9	0.12	F
2-4	34	31	3		
B symptoms					
yes	51	43	8	1	F
no	24	20	4		
IPI group					
0-2	17	12	5	0.12	F
3-5	60	53	7		
First line chemotherapy					
anthracyclin based	59	49	10	1	Khi2
others	17	15	2		
Frontline auto SCT					
yes	9	7	2	0.59	F
no	58	51	7		
5 years OS	35%	37%	25%	0.88	log rank
Response to treatment*					
CR	34	27	7	0.49	F
PR	11	9	2		
SD	0	0	0		
PD	8	8	0		
Early progression*					
yes	13	12	1	0.43	F
no	46	37	9		
5 years OS*	39%	43%	20%	0.5	log rank
5 years PFS *	27%	30%	10%	0.35	log rank

*** anthracyclin based chemotherapy**

Table S2. Summary of the clinical features of the 85 patients of the extended cohort (72 AITL and 13 TFH-like PTCL cases).

Hypergammaglobulinemia is defined as gammaglobukin level>16 g/L.
SCT:stem cell transplantation.
CR complete response, PR partial response, SD stable disease, PD progressive disease.
F: Fisher, MW: Mann Whitney

DELETIONS				
deleted region #	**Chromosome**	**localization (bp)**		**Patient ID**
MCR1	1	1 600 000	1 775 000	TENOM04.119
				TENOM04.026
MCR2	2	203 100 000	204 000 000	TENOM04.119
				TENOM04.026
MCR3	3	48 950 000	49 176 000	TENOM04.119
				TENOM04.121
MCR4	7	4 700 000	5 970 000	TENOM04.119
				TENOM04.121
MCR5	7	100 330 000	102 098 000	TENOM04.119
				TENOM04.026
MCR6	8	PVT1 locus		TENOM04.119
				TENOM04.121
MCR7	9	CDKN2A		TENOM04.119
				TENOM04.121
MCR8	12	12 300 000	12 985 000	TENOM04.119
				TENOM04.026
				TENOM04.121

Table S3. Summary of minimal common regions (MCR) deleted in at least two of ten AITL patients with whole-genome/whole-exome sequencing (discovery cohort)

GENE	Pathway	GENE ID	Chr	Patient ID	mutation	Position	Reference allele	Alternate allele	VF (%)
CDK11B	Cell Cycle	ENSG00000248333	1	TENOM04.026	Deletion; Homo				
CDK11B	Cell Cycle	ENSG00000248333	1	TENOM04.119	Deletion; Homo				
CDKN1B	Cell Cycle	ENSG00000111276	1	TENOM04.026	Deletion; Homo				
CDKN1B	Cell Cycle	ENSG00000111276	1	TENOM04.119	Deletion; Homo				
CDKN1B	Cell Cycle	ENSG00000111276	1	TENOM04.121	Deletion; Homo				
MTOR	TCR signalling	ENSG00000198793	1	TENOM04.119	R2430T	11174386	C	G	20.8
CEP170	Cell Cycle	ENSG00000143702	1	TENOM04.115	T378I	243329049	G	A	24
CEP170	Cell Cycle	ENSG00000143702	1	TENOM 04.026	Gain; Het				
CEP170	Cell Cycle	ENSG00000143702	1	TENOM 04.119	Gain; Het				
DHX9	mRNA processing	ENSG00000135829	1	TENOM04.065	E629Q	182845254	G	C	28.7
DHX9	mRNA processing	ENSG00000135829	1	TENOM 04.026	Gain; Het				
DHX9	mRNA processing	ENSG00000135829	1	TENOM 04.119	Gain; Het				
DOCK7	TCR signalling	ENSG00000116641	1	TENOM 04.026	Deletion; Het				
DOCK7	TCR signalling	ENSG00000116641	1	TENOM 04.119	R1550K	62970323	C	T	53
DYRK3	Epignetic	ENSG00000143479	1	TENOM04.065	V465L	206821936	G	T	25.4
DYRK3	Epignetic	ENSG00000143479	1	TENOM 04.026	Gain; Het				
DYRK3	Epignetic	ENSG00000143479	1	TENOM 04.119	Gain; Het				
HMCN1		ENSG00000143341	1	TENOM 04.026	Gain; Het				
HMCN1		ENSG00000143341	1	TENOM 04.119	K1027T	185958651	A	C	28
HMCN1		ENSG00000143341	1	TENOM 04.119	Gain; Het				
JAK1	JAK_STAT signalling	ENSG00000162434	1	TENOM04.026	G1097D	65301158	C	T	30
KCNK2		ENSG00000082482	1	TENOM 04.026	Gain; Het				
KCNK2		ENSG00000082482	1	TENOM 04.119	Y272D	215345517	T	G	19
KCNK2		ENSG00000082482	1	TENOM 04.119	Gain; Het				
MIA3		ENSG00000154305	1	TENOM04.065	S725X	222838777	C	A	22.3
MIA3		ENSG00000154305	1	TENOM 04.026	Gain; Het				
MIA3		ENSG00000154305	1	TENOM 04.119	Gain; Het				
NEK2	Cell Cycle	ENSG00000117650	1	TENOM04.115	L376F	211840431	C	A	35.4
NEK2	Cell Cycle	ENSG00000117650	1	TENOM 04.026	Gain; Het				
NEK2	Cell Cycle	ENSG00000117650	1	TENOM 04.119	Gain; Het				
TOR1AIP2		ENSG00000169905	1	TENOM04.065	Q10P	179821772	T	G	47.6
TOR1AIP2		ENSG00000169905	1	TENOM 04.026	Gain; Het				
TOR1AIP2		ENSG00000169905	1	TENOM 04.119	Gain; Het				
TRAF5	TCR signalling	ENSG00000082512	1	TENOM04.115	N18I	211526634	A	T	50
TRAF5	TCR signalling	ENSG00000082512	1	TENOM 04.026	Gain; Het				
TRAF5	TCR signalling	ENSG00000082512	1	TENOM 04.119	Gain; Het				
DOCK10	TCR signalling	ENSG00000135905	2	TENOM04.115	V1038L	225688289	C	A	43.4
DOCK10	TCR signalling	ENSG00000135905	2	TENOM04.026	P903S	225704744	G	A	37
FSIP2		ENSG00000188738	2	TENOM04.026	R309C	186611436	C	T	28
FSIP2		ENSG00000188738	2	TENOM04.119	I688L	186653658	A	C	24
FSIP2		ENSG00000188738	2	TENOM04.119	I5382L	186669910	A	C	47
FSIP2		ENSG00000188738	2	TENOM04.119	K6078T	186671999	A	C	19
RHOA	TCR signalling	ENSG00000067560	3	TENOM04.026	G17V	49412973	C	A	26
RHOA	TCR signalling	ENSG00000067560	3	TENOM28.001	G17V	49412973	C	A	18
RBP7		ENSG00000162444	3	TENOM 04.119	Deletion; Het				
RBP7		ENSG00000162444	3	TENOM04.026	Deletion; Het				
CTNNB1	TCR signalling	ENSG00000168036	3	TENOM04.026	G34E	41266104	G	A	15
TET2	Epignetic	ENSG00000168769	4	TENOM04.120	Q1034X	106193748	C	T	21
TET2	Epignetic	ENSG00000168769	4	TENOM04.120	R206X	106413197	C	T	21
TET2	Epignetic	ENSG00000168769	4	TENOM07.025	G898X	106157791	G	T	9
TLR6	TLR signalling	ENSG00000174130	4	TENOM04.065	D610Y	38829267	C	A	32.9
TLR6	TLR signalling	ENSG00000174130	4	TENOM 04.119	Gain; Het				
WDFY3	Autophagy	ENSG00000163625	4	TENOM04.065	L1721F	85686988	T	A	33.7
WDFY3	Autophagy	ENSG00000163625	4	TENOM 04.119	M1299T	85708640	A	G	30
WDFY3	Autophagy	ENSG00000163625	4	TENOM 04.119	K488T	85742365	T	G	38
DNAH8		ENSG00000124721	6	TENOM04.06	I3597T	38899753	T	C	26.5
DNAH8		ENSG00000124721	6	TENOM04.119	R3949X	38939412	C	T	45
FYN	TCR signalling	ENSG00000010810	6	TENOM 04.119	Deletion; homo				
FYN	TCR signalling	ENSG00000010810	6	TENOM04.026	Deletion; Het				
MDN1		ENSG00000112159	6	TENOM04.065	D364Y	90499886	C	A	19.5
MDN1		ENSG00000112159	6	TENOM 04.119	D4565N	90382020	C	T	54
MDN1		ENSG00000112159	6	TENOM04.026	Deletion; Het				
GTF2I	TCR signalling	ENSG00000077809	7	TENOM04.081	L607F	74159167	G	C	22.9
GTF2I	TCR signalling	ENSG00000077809	7	TENOM 04.119	Deletion; Het				
GTF2I	TCR signalling	ENSG00000077809	7	TENOM04.121	Deletion; Het				
SPDYE2		ENSG00000205238	7	TENOM04.081	F94L	102198956	T	C	21.5
SPDYE2		ENSG00000205238	7	TENOM 04.026	Gain; Het				
SPDYE2		ENSG00000205238	7	TENOM 04.121	Gain; Het				
PVT1		ENSG00000249859	8	TENOM04.119	Deletion; Homo				
PVT1		ENSG00000249859	8	TENOM04.121	Deletion; Homo				
CDKN2A	Cell Cycle	ENSG00000147889	9	TENOM04.119	Deletion; Homo				
CDKN2A	Cell Cycle	ENSG00000147889	9	TENOM04.121	Deletion; Homo				
DDX58	mRNA processing	ENSG00000107201	9	TENOM04.081	D502Y	32467832	C	A	40.9
DDX58	mRNA processing	ENSG00000107201	9	TENOM04.026	M204T	32491379	A	G	14
DMBT1		ENSG00000187908	10	TENOM04.065	S643P	124361393	T	C	39.2
DMBT1		ENSG00000187908	10	TENOM04.119	S1052T	124358487	T	A	50
DMBT1		ENSG00000187908	10	TENOM04.121	Deletion; Het				
CREBL2	TCR signalling	ENSG00000111269	12	TENOM04.026	Deletion; Homo				
CREBL2	TCR signalling	ENSG00000111269	12	TENOM04.119	Deletion; Homo				
CREBL2	TCR signalling	ENSG00000111269	12	TENOM04.121	Deletion; Homo				
DUSP16	TCR signalling	ENSG00000111266	12	TENOM04.026	Deletion; Homo				
DUSP16	TCR signalling	ENSG00000111266	12	TENOM04.119	Deletion; Homo				
DUSP16	TCR signalling	ENSG00000111266	12	TENOM04.121	Deletion; Homo				
LRP6	Wint signalling	ENSG00000070018	12	TENOM04.026	Deletion; Homo				
LRP6	Wint signalling	ENSG00000070018	12	TENOM04.119	Deletion; Homo				
LRP6	Wint signalling	ENSG00000070018	12	TENOM04.119	E180V	12356245	T	A	42
LRP6	Wint signalling	ENSG00000070018	12	TENOM04.121	Deletion; Homo				
PIK3C2G	TCR signalling	ENSG00000139144	12	TENOM04.065	V453A	18491445	T	C	23.3
GOLGA8B		ENSG00000215252	15	TENOM04.081	T132I	34823738	G	A	25.4
GOLGA8B		ENSG00000215252	15	TENOM 028.001	Gain; Het				
GOLGA8B		ENSG00000215252	15	TENOM 04.060	Gain; Het				
CREBBP	TCR signalling	ENSG00000005339	16	TENOM04.119	Deletion; Homo				
KRT20		ENSG00000171431	17	TENOM 04.060	Gain; Het				
KRT20		ENSG00000171431	17	TENOM 04.119	E406D	39032670	T	G	46
NLRP4	Autophagy	ENSG00000160505	19	TENOM04.065	T162M	56369244	C	T	28.4
NLRP4	Autophagy	ENSG00000160505	19	TENOM04.119	R810H	56382267	G	A	25
TPRX1		ENSG00000178928	19	TENOM 04.119	Deletion; Het				
TPRX1		ENSG00000178928	19	TENOM04.121	Deletion; Het				
VAV1	TCR signalling	ENSG00000141968	19	TENOM04.119	R822Q	6805090	G	A	91
IFNAR2	IFNgamma signalling	ENSG00000159110	21	TENOM 04.026	Gain; Het				
IFNAR2	IFNgamma signalling	ENSG00000159110	21	TENOM 04.121	W54X	34617320	G	A	18
IFNAR2	IFNgamma signalling	ENSG00000159110	21	TENOM 08.001	Gain; Het				
F8		ENSG00000185010	X	TENOM04.065	A68V	154090108	G	A	28.8
F8		ENSG00000185010	X	TENOM 04.119	K1459T	153810883	T	G	
F8		ENSG00000185010	X	TENOM 04.119	Gain; Het				
MAGEC1		ENSG00000155495	X	TENOM 04.119	S535G	140994793	A	G	81
MAGEC1		ENSG00000155495	X	TENOM 04.119	Gain; Het				
MAGEC1		ENSG00000155495	X	TENOM 04.121	Gain; Het				
BEND2		ENSG00000177324	X	TENOM04.026	M572L	18194130	T	A	22
BEND2		ENSG00000177324	X	TENOM04.065	N542Y	18192234	T	A	24.9

Table S4. Significant gene alterations found in the discovery cohort. Summary of SNVs and CNVs of 39 genes altered in at least two patients of 10 AITL patients subject to WG/ES and variants in 6 genes related to TCR signaling pathway found mutated in one patient each. Genes are arranged by chromosome number and position. Variants are presented according to GRCh37 assembly (Ensembl). VF: Variant frequency; Chr: chromosome; Homo:homozygous; Het: heterozygous

HGVS name	ensembl #	localization (chr:start-end:strand)	targeted	function	pathway
AKT1	ENSG00000142208	14:105235686-105262088:-1	exons	kinase	TCR signalling
AKT2	ENSG00000105221	19:40736224-40791443:-1	exons	kinase	TCR signalling
BCL6	ENSG00000113916	3:187439165-187463515:-1	exons	transcription factor	TCR signalling
BRAF	ENSG00000157764	7:140,419,127-140,624,564:-1	exons	kinase	TCR signalling
CARD11	ENSG00000198286	7:2,945,775-3,083,579:-1	exons		TCR signalling
CD28	ENSG00000178562	2:204571198-204602557:+1	exons	receptor	TCR signalling
CDC42	ENSG00000070831	1:22379120-22419437:+1	exons	small GTPase	TCR signalling
CDK11B	**ENSG00000248333**	**1:1570603-1590473:-1**	**exons**	**cyclin**	**Cell Cycle**
CDKN1B	**ENSG00000111276**	**12:12867992-12875305:+1**	**exons**	**cyclin inhibitor**	**Cell Cycle**
CDKN2A	**ENSG00000147889**	**9:21967751-21995300:-1**	**exons**	**cyclin inhibitor**	**Cell Cycle**
CEP170	**ENSG00000143702**	**1:243287730-243418650:-1**	**exons**	**centrosome component**	**Cell Cycle**
CREBBP	**ENSG00000005339**	**16:3775055-3930727:-1**	**exons**	**transcription factor**	**TCR signalling**
CREBL2	**ENSG00000111269**	**12:12764761-12798042:+1**	**exons**	**transcription factor**	**TCR signalling**
CTNNB1	**ENSG00000168036**	**3:41236328-41301587:+1**	**exons**	**transcription factor**	**TCR signalling**
CTNND1	ENSG00000198561	11:57520715-57587018:+1	exons	GAP	TCR signalling
DDX58	**ENSG00000107201**	**9:32455300-32526322:-1**	**exons**	**RNA helicase**	**mRNA processing**
DHX9	**ENSG00000135829**	**1:182808504-182856886:+1**	**exons**	**RNA helicase**	**mRNA processing**
DMBT1	**ENSG00000187908**	**10:124320181-124403252:+1**	**exons**	**transcription factor**	**unknown**
DOCK10	**ENSG00000135905**	**2:225629807-225907162:-1**	**exons**	**GEF**	**TCR signalling**
DOCK5	ENSG00000147459	8:25042238-25275598:+1	exons	GEF	TCR signalling
DOCK7	**ENSG00000116641**	**1:62920399-63153969:-1**	**exons**	**GEF**	**TCR signalling**
DUSP16	**ENSG00000111266**	**12:12628829-12715317:-1**	**exons**	**MAPK phosphatase**	**TCR signalling**
DYRK2	ENSG00000127334	12:68042118-68059186:+1	exons	kinase	Epigenetic
DYRK3	**ENSG00000143479**	**1:206808881-206857764:+1**	**exons**	**kinase**	**Epigenetic**
FYN	**ENSG00000010810**	**6:111981535-112194655:-1**	**exons**	**kinase**	**TCR signalling**
GSK3β	ENSG00000082701	3:119540170-119813264:-1	exons	kinase	TCR signalling
GTF2I	**ENSG00000077809**	**7:74071994-74175026:+1**	**exons**	**transcription factor**	**TCR signalling**
ICOS	ENSG00000163600	2:204801471-204826300:+1	exons	receptor	TCR signalling
IFNAR2	**ENSG00000159110**	**21:34602206-34637969:+1**	**exons**	**receptor**	**Receptor**
IRF4	ENSG00000137265	6:391739-411447:+1	exons	transcription factor	TCR signalling
ITK	ENSG00000113263	5:156569944-156682201:+1	exons	kinase	TCR signalling
JAK1	**ENSG00000162434**	**1:65,298,912-65,432,187:-1**	**hotspots**	**kinase**	**JAKs_STATs signalling**
JAK2	ENSG00000096968	9:4,985,033-5,128,183:+1	hotspots	kinase	JAKs_STATs signalling
JAK3	ENSG00000105639	9:17,935,589-17,958,880:-1	hotspots	kinase	JAKs_STATs signalling
KRAS	ENSG00000133703	12:25,357,723-25,403,870:-1	exons	kinase	TCR signalling
LAT	ENSG00000213658	16:28,984,826-28,990,783:+1	exons	molecular bridge	TCR signalling
LCK	ENSG00000182866	1:32716840-32751766:+1	exons	kinase	TCR signalling
LRP6	**ENSG00000070018**	**12:12268959-12419946:-1**	**exons**	**co-receptor**	**Wint signalling**
MAF	ENSG00000178573	16:79619740-79634611:-1	exons	transcription factor	TCR signalling
MAPK1	ENSG00000100030	22:22108789-22221970:-1	exons	kinase	TCR signalling
MAPK3	ENSG00000102882	16:30125426-30134827:-1	exons	kinase	TCR signalling
MAPK8	ENSG00000107643	10:49514698-49647403:+1	exons	kinase	TCR signalling
MAPK9	ENSG00000050748	5:179660143-179719099:-1	exons	kinase	TCR signalling
MDN1	**ENSG00000112159**	**6:90352218-90529442:-1**	**exons**	**nuclear chaperonne**	**nuclear chaperonne**
MYD88	ENSG00000172936	3:38,179,969-38,184,513:+1	hotspots	adaptor protein	TLR signalling
NEK2	**ENSG00000117650**	**1:211836114-211848960:-1**	**exons**	**kinase**	**Cell Cycle**
NEK6	ENSG00000119408	9:127019885-127115586:+1	exons	kinase	Cell Cycle
NLRP4	**ENSG00000160505**	**19:56347944-56393220:+1**	**exons**	**pattern recognition receptor**	**Autophagy**
PDPK1	ENSG00000140992	16:2587965-2653189:+1	exons	kinase	TCR signalling
PIK3CA	ENSG00000121879	3:178865902-178957881:+1	exons	PIK3 catalytic subunit	TCR signalling
PIK3CB	ENSG00000051382	3:138372860-138553780:-1	exons	PIK3 catalytic subunit	TCR signalling
PIK3CG	ENSG00000105851	7:106505723-106547590:+1	exons	PIK3 catalytic subunit	TCR signalling
PIK3R1	ENSG00000145675	5:67511548-67597649:+1	exons	PIK3 regulatory subunit	TCR signalling
PIK3R5	ENSG00000141506	17:8782233-8869029:-1	exons	PIK3 regulatory subunit	TCR signalling
PLCG1	ENSG00000124181	20:39765600-39825427:+1	exons	kinase	TCR signalling
PLCG2	ENSG00000197943	16:81772702-81991899:+1	exons	kinase	TCR signalling
PRKCQ	ENSG00000065675	10:6,469,105-6,622,263:-1	exons	kinase	TCR signalling
RAC1	ENSG00000136238	7:6414154-6443608:+1	exons	small GTPase	TCR signalling
RHOA	**ENSG00000067560**	**3:49396578-49450431:-1**	**exons**	**small GTPase**	**TCR signalling**
STAT3	ENSG00000168610	17:40,465,342-40,540,586:-1	hotspots	transcription factor	TCR and JAKs_STATs signalling
STAT4	ENSG00000138378	2:191,894,302-192,016,322:-1	hotspots	transcription factor	JAKs_STATs signalling
STAT5B	ENSG00000173757	17:40,351,186-40,428,725:-1	hotspots	transcription factor	JAKs_STATs signalling
TPRX1	**ENSG00000178928**	**19:48304500-48322308:-1**	**exons**	**transcription factor**	**Transcription factor**
TRAF5	**ENSG00000082512**	**1:211499957-211548288:+1**	**exons**	**scaffold protein**	**TCR signalling**
TRAF6	ENSG00000175104	11:36,508,577-36,531,822:-1	exons	E3 ubiquitin ligase	TCR signalling
VAV1	**ENSG00000141968**	**19:6772725-6857377:+1**	**exons**	**GEF**	**TCR signalling**
VAV2	ENSG00000160293	9:136627016-136857726:-1	exons	GEF	TCR signalling
WDFY3	**ENSG00000163625**	**4:85590704-85887544:-1**	**exons**	**scaffold protein - PIP3 binding prot**	**Autophagy**
ZAP70	ENSG00000115085	2:98,330,023-98,356,325:+1	exons	kinase	TCR signalling

Table S5. List of 69 genes analyzed by targeted deep sequencing. The 27 genes in boldface were selected from WG/ES of the discovery cohort**.** Genes found alteres in whole genome / whole exome sequencing are in bold face.

GENE	uniprot #	#CHROM	POSITION	ID	Nucleotide Change	Amino Acid Change	Mutation type	domain	somatic in cosmic	VF (mean)	VF (min)	VF (max)	# (AITL)	# (TFH-like)	Filtered out	SIFT	PROVEAN	Polyphen-2
CDK11B	P21127	1	1577072	.	NM_033489:exon10:c.846_851del	282_284del	non frameshift deletion	Glu rich domain		0.19	0.19	0.19	1	0		NA	NA	NA
JAK1	P23458	1	65307195	.	NM_002227:exon18:c.2493C>A	D831E	missense	kinase domain			0.05	0.05	0	1		Deleterious	Damaging	probably damaging
LCK	P06239	1	32751125	.	[b:]NM_001042771:exon13:c.1338C>A	[b:]N446K	missense	kinase domain		0.26	0.26	0.26	1	0		Neutral	Tolerated	probably damaging
LCK		1	32751127	.	[b:]NM_001042771:exon13:c.1340C>G:p.P447R	[b:]P447R	missense	kinase domain		0.26	0.26	0.26	1	0		Deleterious	Damaging	probably damaging
DOCK7	Q96N67	1	63042973	.	NM_033407:exon18:c.2072T>C	L691S	missense	DHR-1 domaim		0.48	0.48	0.48	0	1	yes	Neutral	Tolerated	probably damaging
DYRK3	O43781	1	206811055	.	NM_003582:exon2:c.138T>G	C46W	missense			0.53	0.53	0.53	1	0	yes	Neutral	Tolerated	probably damaging
TRAF5	O00463	1	211526601	.	:NM_145759:exon2:c.20A>G	H7R	missense			0.53	0.53	0.53	0	1	yes	Deleterious	Damaging	benign
CEP170	Q5SW79	1	243362476	.	NM_001042404:exon7:c.517G>T	G173C	missense			0.04	0.04	0.04	1	0		Neutral	Tolerated	possibly damaging
CD28	P10747	2	204591674	.	NM_006139:exon2:c.371A>T	D124V	missense	extracellular		0.12	0.09	0.16	2	0		Neutral	Tolerated	possibly damaging
CD28		2	204591675	.	NM_006139:exon2:c.372C>A	D124E	missense	extracellular		0.11	0.07	0.12	2	0		Neutral	Tolerated	possibly damaging
CD28		2	204599555	.	NM_006139:exon4:c.583A>C	T195P	missense	cytoplasmic		0.24	0.11	0.38	4	0		Deleterious	Damaging	benign
MYD88	P22366	3	38182032	.	NM_001172567:exon3:c.656C>G	S219C	missense	TIR domain	yes	0.40	0.40	0.40	0	1		Deleterious	Damaging	possibly damaging
CTNNB1	P35222	3	41266124	.	[a:] NM_001904:exon3:c.122A>G	[a:] T41A	missense	Phospho by GSK3b	yes	0.09	0.05	0.12	1	1		Deleterious	Damaging	possibly damaging
CTNNB1		3	41266110	.	NM_001904:exon3:c.107A>C	H36P	missense		yes	0.15	0.15	0.15	1	0		Deleterious	Damaging	possibly damaging
CTNNB1		3	41266137	.	[a:] NM_001904:exon3:c.134C>T	[a:] S45F	missense		yes	0.03	0.03	0.03	2	0		Deleterious	Damaging	possibly damaging
CTNNB1		3	41268766	.	NM_001904:exon7:c.1004A>C	K335T	missense		yes	0.13	0.08	0.17	2	0		Deleterious	Damaging	possibly damaging
RHOA	P61586	3	49412969	.	NM_001664:exon2:c.54G>T	K18N	missense	GTP binding		0.08	0.06	0.10	3	0		Deleterious	Damaging	possibly damaging
RHOA		3	49412973	rs11552761	NM_001664:exon2:c.50G>T	G17V	missense	GTP binding	yes	0.15	0.02	0.39	42	6		Neutral	Tolerated	possibly damaging
PIK3CB	P42338	3	138433476	.	NM_006219:exon7:c.1136A>G	H379R	missense	C2 PI3K-type		0.50	0.50	0.50	1	0	yes	Deleterious	Damaging	possibly damaging
PIK3CA	P42336	3	178951947	.	NM_006218:exon21:c.3002T>C	L1001P	missense	PI3K/PI4K		0.02	0.02	0.02	0	1		Deleterious	Damaging	possibly damaging
WDFY3	Q8IZQ1	4	85758240	.	NM_014991:exon7:c.418A>C:	T140P	missense			0.09	0.09	0.09	1	0		Neutral	Tolerated	possibly damaging
PIK3R1	P27986	5	67569305	.	NM_181523exon3:c.422A>G	K141R	missense	RHO-GAP		0.02	0.02	0.02	0	1		Deleterious	Damaging	benign
PIK3R1		5	67589661	.	NM_181523:exon11:c.1424A>C	Q475P	missense	iSH2		0.02	0.02	0.02	1	0		Neutral	Tolerated	possibly damaging
PIK3R1		5	67591133	.	NM_181523:exon13:c.1726A>G	T576A	missense	iSH2		0.02	0.02	0.02	0	1		Deleterious	Damaging	benign
PIK3R1		5	67593292	.	NM_181523:exon16:c.2038G>A	G680S	missense	SH2 2		0.04	0.04	0.04	0	1		Neutral	Damaging	possibly damaging
PIK3R1		5	67593364	.	NM_181523:exon16:c.2110G>A	V704M	missense	SH2 2		0.04	0.04	0.04	1	0		Deleterious	Damaging	possibly damaging
IRF4	Q15306	6	394867	rs202124383	NM_002460:exon3:c.263C>A	P88Q	missense	DNA binding		0.48	0.48	0.48	1	0	yes	Deleterious	NA	possibly damaging
MDN1	Q9NU22	6	90372565	.	NM_014611:exon86:c.14355_14357del	4785_4786del	non frameshift deletion	poly glu		0.43	0.43	0.43	1	0	yes	NA	NA	NA
MDN1		6	90415827	.	NM_014611:exon53:c.8099T>C	L2700P	missense			0.51	0.51	0.51	1	0	yes	Deleterious	Tolerated	possibly damaging
MDN1		6	90428552	.	M_014611:exon42:c.6255C>G	H2085Q	missense	near ATP binding		0.39	0.39	0.39	1	0		Neutral	Tolerated	benign
MDN1		6	90481323	.	NM_014611:exon15:c.2101G>A	V701I	missense	near ATP binding		0.11	0.11	0.11	0	1		Deleterious	Damaging	benign
MDN1		6	90482411	.	NM_014611:exon14:c.1964C>T	P655L	missense	near ATP binding		0.50	0.50	0.50	1	0	yes	NA	NA	benign
FYN	P06241	6	111982968	.	NM_153047:exon11:c.1579C>T	Q527X	stop gain			0.05	0.05	0.06	1	0		NA	NA	possibly damaging
FYN		6	111982971	.	[a:]NM_153047:exon11:c.1574_1575del	[a:]525_525del	frameshift deletion			0.07	0.07	0.07	0	1		Deleterious	Damaging	NA
FYN		6	112024228	.	[a:]NM_153047:exon5:c.557C>T	[a:]S186L	missense	SH2 domain		0.16	0.16	0.16	0	1		NA	NA	possibly damaging
FYN		6	112035569	.	[b:] NM_153047:exon2:c.324delA	[b:] K108fs	frameshift deletion			0.10	0.10	0.10	1	0		Deleterious	Damaging	possibly damaging
FYN		6	112035573	.	[b:] NM_153047:exon2:c.321AAG>TCT	[b:] E107S	missense	SH3 domain		0.10	0.10	0.10	1	0		Deleterious	Damaging	possibly damaging
CARD11	Q9BXL7	7	2955005	.	NM_032415:exon21:c.2705T>G	F902C	missense			0.06	0.06	0.06	1	0		Neutral	Damaging	possibly damaging
CARD11		7	2969640	.	NM_032415:exon12:c.1639T>A	S547T	missense			0.05	0.05	0.05	0	1		Deleterious	Damaging	benign
CARD11		7	2984003	.	NM_032415:exon5:c.527T>G	F176C	missense	coiled coil		0.49	0.49	0.49	1	0		Neutral	Tolerated	possibly damaging
GTF2I	P78347	7	74143131	.	NM__032999:exon13:c.951T>G	D317E	missense			0.17	0.17	0.17	1	0		Neutral	Tolerated	benign
GTF2I		7	74143199	.	NM_032999:exon13:c.1019A>G	N340S	missense			0.21	0.21	0.21	0	1		Neutral	Tolerated	benign
GTF2I		7	74150975	.	NM__032999:exon18:c.1569G>T	R523S	missense	GTF2I-like		0.17	0.17	0.17	1	0		Neutral	Damaging	possibly damaging
GTF2I		7	74159167	.	NM_032999:exon21:c.1821G>C	L607F	missense	GTF2I-like	yes	0.25	0.25	0.25	1	0		Neutral	Tolerated	possibly damaging
GTF2I		7	74162388	.	NM_032999:exon24:c.2105G>A	R702Q	missense			0.18	0.18	0.18	1	0		Neutral	Tolerated	benign
PIK3CG	P48736	7	106508166	.	NM_002649:exon2:c.160C>G	P54A	missense	PI3K-ABD		0.49	0.49	0.49	1	0	yes	Neutral	Tolerated	benign
DOCK5	Q9H7D0	8	25240226	.	NM_024940:exon40:c.4063G>T	A1355S	missense	DHR-2 domain		0.49	0.49	0.49	0	1	yes	Neutral	Damaging	benign
CDKN2A	P42771	9	21968733	.	NM_001195132:exon3:c.495G>C	R165S	missense			0.44	0.44	0.44	1	0	yes	Neutral	Tolerated	possibly damaging
DDX58	O95786	9	32488079	.	NM_014314:exon8:c.1076C>T	T359M	missense	Helicase ATP-binding	no	0.48	0.48	0.48	1	0	yes	Deleterious	Damaging	possibly damaging
JAK2	O60674	9	5073770	rs77375493	NM_004972:exon14:c.1849G>T	V617F	missense		yes	0.15	0.15	0.15	1	0		Neutral	Damaging	possibly damaging
VAV2	P52735	9	136674187	.	NM_001134398:exon7:c.641A>G	Y214C	missense	DH domain	yes	0.57	0.57	0.57	1	0		NA	NA	possibly damaging
DMBT1	Q9UGM3	10	124325492	.	NM_017579:exon2:c.72_79del	24_27del	frameshift deletion			0.44	0.44	0.44	1	0	yes	NA	NA	NA
DMBT1		10	124342406	.	NM_017579:exon13:c.1357C>G	Q453E	missense	SRCR 3		0.61	0.61	0.61	1	0	yes	Neutral	Tolerated	possibly damaging
DMBT1		10	124348727	.	NM_017579:exon16:c.2021A>G	N674S	missense	SRCR 5		0.86	0.86	0.86	1	0	yes	Deleterious	Tolerated	benign
DMBT1		10	124366695	.	NM_017579:exon29:c.3658C>T	P1220S	missense	SRCR 9		1.00	1.00	1.00	0	1	yes	NA	NA	benign
TRAF6	Q9Y4K3	11	36511918	.	NM_004620:exon7:c.1039C>T	Q347X	stop gain	coiled coil /MATH		0.14	0.14	0.14	1	0		Neutral	Tolerated	possibly damaging
TRAF6		11	36518706	.	NM_145803:exon5:c.558G>T	Q186H	missense	TRAF-type 1		0.50	0.50	0.50	1	0	yes	Neutral	Tolerated	possibly damaging
LRP6	O75581	12	12278241	.	NM_002336:exon21:c.4438T>A	Y1480N	missense	PPPSP motif A		0.17	0.17	0.17	1	0		Neutral	Tolerated	possibly damaging
LRP6		12	12291358	.	NM_002336:exon16:c.3508A>G	I1170V	missense	LDL-receptor class B 20		0.45	0.45	0.45	1	0	yes	Deleterious	Damaging	benign
LRP6		12	12334271	rs141212743	NM_002336:exon6:c.1079G>A	R360H	missense	Beta-propeller 2		0.51	0.51	0.51	1	0	yes	Neutral	Damaging	possibly damaging
KRAS	P01116	12	25398211	.	NM_004985:exon2:c.108A>G	I36M	missense		no	0.03	0.03	0.03	0	1		Deleterious	Damaging	possibly damaging
KRAS		12	25398266	.	NM_004985:exon2:c.53C>A	A18D	missense	GTP binding	no	0.03	0.03	0.03	1	0		Deleterious	Damaging	possibly damaging
KRAS		12	25398281	.	NM_033360:exon2:c.38G>A	G13D	missense	GTP binding	yes	0.25	0.25	0.25	0	1		Deleterious	Damaging	possibly damaging
AKT1	P31749	14	105239665	.	NM_001014431:exon10:c.880G>A	G294R	missense	protein kinase		0.33	0.33	0.33	1	0		Neutral	NA	possibly damaging
PDPK1	O15530	16	2607734	.	NM_002613:exon2:c.56_58del	19_20del	non frameshift deletion			0.32	0.32	0.32	1	0		NA	NA	NA
PDPK1		16	2611895	.	NM_002613:exon4:c.453_456del	151_152del	frameshift deletion	protein kinase		0.28	0.28	0.28	1	0		Deleterious	Damaging	NA
PDPK1		16	2633432	.	NM_002613:exon10:c.971G>A	R324Q	missense	protein kinase		0.31	0.31	0.31	1	0		Deleterious	Tolerated	possibly damaging
PDPK1		16	2633480	.	NM_002613:exon10:c.1019C>A	P340Q	missense	protein kinase		0.27	0.27	0.27	1	0		Neutral	Tolerated	benign
PDPK1		16	2636756	rs75824263	NM_002613:exon11:c.1205C>T	T402M	missense			0.49	0.19	0.49	1	0	yes	Deleterious	Tolerated	possibly damaging
LAT	O43561	16	28997042	rs55945024	NM_001014989:exon3:c.217G>A	D73N	missense			0.52	0.52	0.52	0	1	yes	Deleterious	Tolerated	possibly damaging
LAT		16	28997459	.	NM_001014989:exon5:c.275C>T	T92M	missense			0.47	0.47	0.47	1	0	yes	Deleterious	Damaging	possibly damaging
CREBBP	Q92793	16	3781835	.	NM_004380:exon29:c.4832C>T	P1611L	missense	Interaction with TRERF1		0.44	0.44	0.44	1	0	yes	Neutral	Damaging	possibly damaging
CREBBP		16	3900638	rs146538907	NM_004380:exon2:c.458C>T	P153L	missense			0.61	0.51	0.71	2	0	yes	Deleterious	Damaging	possibly damaging
MAPK3	P27361	16	30128549	.	NM_001040056:exon6:c.833G>A	R278Q	missense	protein kinase		0.02	0.02	0.02	1	0		Deleterious	Damaging	possibly damaging
MAPK3		16	30129406	.	NM_002746:exon4:c.622C>T	R208C	missense	protein kinase		0.50	0.50	0.50	1	0	yes	Neutral	Tolerated	possibly damaging
PLCG2	P16885	16	81819700	.	NM_002661:exon2:c.106T>C	S36P	missense	PH domain		0.58	0.58	0.58	1	0	yes	Neutral	Damaging	benign

PLCG2		16	81957181	.	NM_002661:exon22:c.2399C>G	S800C	missense	SH3 domain		0.48	0.48	0.48	1	0	yes	Deleterious	Damaging	possibly damaging
STAT3	P40763	17	40475063	.	NM_139276:exon20:c.1847A>G	E616G	missense	SH2 domain	yes	0.03	0.03	0.03	1	0		Deleterious	Damaging	possibly damaging
STAT3		17	40475064	.	NM_139276:exon20:c.1846G>A	E616K	missense	SH2 domain	yes	0.04	0.04	0.04	1	0		Neutral	Tolerated	benign
PIK3R5	Q8WYR1	17	8793325	.	NM_014308:exon8:c.776C>T	A259V	missense		yes	0.53	0.53	0.53	1	0		NA	NA	possibly damaging
VAV1	P15498	19	6822232	.	NM_005428:exon5:c.451_472del	151_158del	frameshift deletion			0.14	0.14	0.14	1	0		Deleterious	Damaging	NA
VAV1		19	6826639	.	NM_005428:exon9:c.844C>T	R282C	missense	DH domain		0.44	0.44	0.44	1	0	yes	NA	NA	possibly damaging
VAV1		19	6853948	.	NM_005428:exon26:c.2333_2348del	778_783del	frameshift deletion			0.06	0.06	0.06	1	0		Deleterious	Damaging	benign
VAV1		19	6854015	.	NM_005428:exon26:c.2390A>G	D797G	missense	SH3 2 domain		0.15	0.15	0.15	1	0		Neutral	Tolerated	possibly damaging
VAV1		19	6854102	.	NM_005428:exon26:c.2477A>C	Y826S	missense	SH3 2 domain		0.07	0.07	0.07	0	1		Neutral	Tolerated	possibly damaging
JAK3	P52333	19	17945764	rs201784993	NM_000215:exon16:c.2096C>T	A699V	missense	kinase domain	yes	0.45	0.45	0.45	1	0		Neutral	Damaging	possibly damaging
TPRX1	Q8N7U7	19	48306003	.	NM_198479:exon2:c.265C>T	P89S	missense			0.44	0.44	0.44	0	1	yes	Deleterious	Damaging	possibly damaging
NLRP4	Q96MN2	19	56369244	rs117212164	NM_134444:exon3:c.485C>T	T162M	missense	NACHT domain	yes	0.48	0.46	0.50	1	1		Deleterious	Damaging	possibly damaging
NLRP4		19	56363459	.	NM_134444:exon2:c.13T>G	F5V	missense	DAPIN domain		0.05	0.05	0.05	0	1		Deleterious	Damaging	possibly damaging
PLCG1	P19174	20	39766420	.	NM_182811:exon1:c.139G>A	E47K	missense	PH 1 domain		0.06	0.06	0.06	0	1		Deleterious	Damaging	possibly damaging
PLCG1		20	39766423	.	NM_182811:exon1:c.142C>T	R48W	missense	PH 1 domain		0.18	0.18	0.18	1	0		Deleterious	Damaging	possibly damaging
PLCG1		20	39792575	.	NM_182811:exon11:c.1025A>G	D342G	missense	PI-PLC X-box domain		0.05	0.05	0.05	0	1		Deleterious	Damaging	possibly damaging
PLCG1		20	39792584	.	[a:] NM_182811:exon11:c.1034C>T	[a:] S345F	missense	PI-PLC X-box domain	yes	0.11	0.04	0.19	1	1		Deleterious	Damaging	possibly damaging
PLCG1		20	39794139	.	[a:] NM_182811:exon15:c.1559C>T	[a:] S520F	missense	PH 2; first part	yes	0.04	0.02	0.04	2	0		Neutral	Tolerated	possibly damaging
PLCG1		20	39795386	.	NM_182811:exon19:c.2188G>A	E730K	missense	SH2 2 domain		0.15	0.15	0.15	1	0		Deleterious	Damaging	possibly damaging
PLCG1		20	39798122	.	NM_002660:exon23:c.2606G>A	G869E	missense	near SH3 domain		0.07	0.03	0.10	2	0		Deleterious	Damaging	possibly damaging
PLCG1		20	39802073	.	NM_182811:exon28:c.3293G>A	R1098Q	missense	C2 domain		0.48	0.48	0.48	1	0	yes	Deleterious	Damaging	possibly damaging
PLCG1		20	39802384	.	NM_182811:exon29:c.3487G>A	E1163K	missense	C2 domain	yes	0.15	0.15	0.15	0	1		Deleterious	Damaging	possibly damaging
PLCG1		20	39802390	.	NM_182811:exon29:c.3493G>C	D1165H	missense	C2 domain		0.37	0.37	0.37	0	1		Deleterious	Damaging	possibly damaging
PLCG1		20	39802391	.	NM_182811:exon29:c.3494A>G	D1165G	missense	C2 domain		0.04	0.04	0.04	1	0		Neutral	Tolerated	possibly damaging
IFNAR2	P48551	21	34619127	.	[a:] NM_207585:exon5:c.326T>C	[a:] V109A	missense	extracellular		0.55	0.55	0.55	1	0	yes	Neutral	Damaging	benign
IFNAR2		21	34635801	rs45513593	[a:] NM_207585:exon9:c.1544G>A	[a:] R515K	missense	cytoplasmique	no	0.54	0.54	0.54	1	0	yes	Neutral	Tolerated	possibly damaging
MAPK1	P28482	22	22161975	rs202041676	NM_138957:exon2:c.280A>G	T94A	missense			0.55	0.55	0.55	1	0	yes	NA	NA	benign

Table S6. List of crossvalidated variants identified by Targeted Deep Sequencing of 69 candidate genes in 85 AITL and TFH-like PTCL samples. 103 variants were found in 45/69 candidate genes analyzed. Genes are arranged by chromosome number and position. Variants are presented according to GRCh37 assembly (Ensembl).

VF: Variant Frequency.

[a]: denotes variants found in the same patient in different alleles.

[b]: denotes variants found in the same patient in the same allele.

Signature name	number of genes	Up	Down	Leading edge genes symbols	Category	Remarks
ABC_gt_GCB_PMBL_MCL_BL_U133AB	51	0.00359964	0.99160084	ABHD17C,PIM2,RAB7L1	T cell activation	
ABCgtGCB_U133AB	273	0.0209979	0.96050395	CKAP4,ABHD17C,FUT8,LARP1B,PIM2,RAB7L1,SCN2A	T cell activation	
ABC_gt_GCB_Affy	20	0.02559744	0.98190181	FUT8,PIM2	T cell activation	
IRF4_myeloma_induced_all	289	0.03019698	0.97530247	ANKRD37,GFPT1,KLK1,MTHFD1L,PDIA4,PDS5A,PIM2	T cell activation	
IRF4_myeloma_induced_direct	37	0.04129587	0.839916008	GFPT1,PIM2	T cell activation	
Blood_Module-1.4_Undetermined	97	0.029997	0.920807919	BTG3,CDCA4,CREM,CYLD,EIF5,EPC1,PTP4A1,ZNF331	T cell activation	
Tcell_PIind_CalciumDefPtdown4x_Feske_Fig4	59	0.0289971	0.923707629	LTA,TMCC2,ZBED2	T cell activation	
Thymic_DP_Tcell_gt_Thymic_SP_CD4+Tcell	102	0.01509849	0.874812519	C17orf67,CD8A,CPVL,E2F7,SH2D1A	T cell activation	
HALLMARK_MTORC1_SIGNALING	197	0.049295071	0.98360164	IFRD1,PLOD2,PSPH,SLC7A11,ELOVL6,CYB5B,RPN1,NUFIP1	T cell activation	
JAK_Up_HBL1	328	0.03039696	0.97130287	HOOK3,KBTBD6,KRT71,MTHFD1L,SLC4A7,SYCN,TMED9	T cell activation	
Tcell_cytokine_induced_IL2_IL7_IL15only	23	0.00729927	0.97140286	LTA	T cell activation	
Tcell_cytokine_induced_PMBC_Bcell_induced	29	0.04489551	0.9740026	CREM,DNAJC3	T cell activation	
HALLMARK_KRAS_SIGNALING_DN	197	0.940605939	0.0169983	MAGIX,ARHGDIG,KCNQ2,SLC30A3,SSTR4,PNMT,TLX1	T cell activation	
E2F3_overexpression_2x_up	135	0.00529947	0.99690031	CDC20B,CRELD2,E2F7,KIAA1804	Proliferation	
Cell_cycle_Cho	508	0.04249575	0.99650035	BMPR1A,TIMMDC1,ELOVL6,EPC1,ETV1,FUT8,KLF5,LRRC8B,MOGAT2,NF2,PTPRR,STAM2,SYNGAP1,XIAP,ZFAND5	Proliferation	
T_cell	14	0.9310138	0.101257748	SH2D1A	Proximal TCR signalling elements	Marginal significance

Table S7. L**eading edge genes from GSEA analysis comparing GEP profiles of samples according to the mutational status for TCR signaling genes (mutated versus wild type).** The p-values for upregulated (Up) and downregulated (Down) pathways in patients harbouring mutations are reported, together with the genes with the highest correlation to the mutation status ("Leading edge genes"); genes indicated in boldface are differentially expressed in TCR_Mut versus TCR_WT cases.

												Patient 1		Patient 2		Patient 3		Patient 4	
												WES	WES	TDS	TDS	TDS	TDS	TDS	TDS
												diagnostic	efractory (2.5	diagnostic	refarctory (1)	diagnostic	relapse (13)	diagnostic	relapse (7)
#CHROM	GENE	POSITION	REF	ALT	ID	CHANGE	effect	domain	somatic in cosmic	Filtered out									
4	*TET2*	.	.	.	.	c. 1516insG:p.Cys484fs	frameshift	.	.	.				8.06	7.74				
4	*TET2*	.	.	.	.	c.2937_2938insA:p.Gln958fs	frameshift	.	.	.						ND	ND	NA	NA
4	*TET2*	106180929	.	TTG	T	.	splicing	.	.	.		5.90	5.90						
4	*TET2*	106157791	.	G	T	NM_001127208:exon3:c.2692G>T:p.G898X	stopgain	.	.	.		6.35	6.35						
2	*DNMT3A*					c.2982C>T:p.Arg882Cys	missense	.	.	.				14.23	29.18	ND	ND		
2	*DNMT3A*					p.P700L	missense	.	.	.						ND	ND	NA	NA
15	*IDH2*					c.600A>G:p.Arg172Gly	missense	.	.	.				13.26	13.89	ND	ND		
2	*CD28*	204591675	C	A	.	NM_006139:exon2:c.372C>A:p.D124E	missense	extracellular	.	.						7.4	11.96		
3	*CTNNB1*					NM_001904:exon8:c.1147T>A:p.W383R	missense	.	yes	.									3.58
3	*RHOA*	49412969	C	A	.	NM_001664:exon2:c.54G>T:p.K18N	missense	GTP binding	.	.								7.42	8.44
3	*RHOA*	49412973	C	A	rs11552761	NM_001664:exon2:c.50G>T:p.G17V	missense	GTP binding	yes	.				21.98	22.00	8.98	12.31		
6	*FYN*	111982968	G	A	.	NM_153047:exon11:c.1579C>T:p.Q527X	stop gain	.	.	.				4.95	6.00				
7	*GTF2I*	74150975	G	T	.	NM_032999:exon18:c.1569G>T:p.R523S	missense	.	.	.								17.16	19.10
9	*CDKN2A*	21968733	C	G	.	NM_001195132:exon3:c.495G>C:p.R165S	missense			yes								44.33	48.25
16	*CREBBP*	3781878	T	C	.	NM_004380:exon29:c.4789A>G:p.K1597E	missense	modified residue N6-acetyllysine	.	.							3.00		
19	*NLRP4*	56369244	C	T	rs117212164	NM_134444:exon3:c.485C>T:p.T162M	missense	NACHT domain	yes	.						46.53	46.07		
20	*PLCG1*	39792584	C	T	.	NM_182811:exon11:c.1034C>T:p.S345F	missense	PI-PLC X-box domain	yes	.		6.25	6.25	3.70	4.00				
20	*PLCG1*	39794139	C	T	.	NM_182811:exon15:c.1559C>T:p.S520F	missense	PH 2; first part	yes	.				4.48	4.00				

Table S8. Targeting Deep sequencing of 4 patients with paired samples . One patient from the discovery cohort (patient 1) and three patients from the extended cohort (patients 2 to 4) had samples harvested at diagnosis and in refractory state (patients 1 and 2, at 2.5 and 1 months) or at relapse (patients 3 and 4, at 13 and 7 months). Samples from patients 2 to 4 were TDS using the panels from the extended cohort. Data for *TET2* , *DNMT3A* and *IDH2* are from a previous study. Both samples from patient 1 were TDS using the same panels as for the extended cohort plus a modified panel comprising *TET2* , *DNMT3A* and *IDH2* . Numbers indicate the Variant Frequency, while colors indicate the type of mutation (red: missense; brown: stop gain; blue: freameshift deletion). ND: not determined; NA: not applicable.

TCR-related genes mutations	mutant		WT		statistics	
N	42		43		p value	test
sex						
male	26	62%	24	56%	0.66	F
female	16	38%	19	44%		
median age (quartile)	67	54-75	64	58-71	0.46	F
diagnosis						
AITL	36	86%	36	84%	1	MW
TFH like PTCL	6	14%	7	16%		
stage						
I	0	0%	0	0%	0.45	F
II	0	0%	1	3%		
III	12	32%	9	23%		
IV	26	68%	30	75%		
LDH						
>N	29	78%	23	64%	0.2	F
≤N	8	22%	13	36%		
hemoglobin						
<10 g/dL	11	32%	10	30%	1	F
≥10 g/dL	23	68%	23	70%		
platelets						
<100000	3	9%	1	3%	0.62	F
≥100000	31	91%	29	97%		
hypergammaglobulinemia						
yes	12	48%	9	45%	1	F
no	13	52%	11	55%		
Direct coombs test						
positive	12	57%	16	67%	0.55	F
negative	9	43%	8	33%		
ECOG						
0-1	19	50%	20	57%	0.64	F
2-4	19	50%	15	43%		
B symptoms						
yes	25	68%	26	68%	1	F
no	12	32%	12	32%		
IPI						
0-2	6	16%	11	28%	0.27	F
3-5	32	84%	28	72%		
First line chemotherapy						
anthracyclin based	33	89%	26	67%	0.03	Khi2
Others	4	11%	13	33%		
Frontline auto SCT						
yes	4	10%	5	13%	0.73	F
no	35	90%	33	87%		
5 years OS	29%		43%		0.36	log rank
Response to treatment*						
CR	16	57%	18	72%	0.11	
PR	5	18%	6	24%		
SD	0	0%	0	0%		
PD	7	25%	1	4%		
Early progression *						
yes	11	33%	2	8%	0.02	F
no	22	67%	24	92%		
5 years OS*	33%		46%		0.56	log rank
5 years PFS *	21%		24%		0.11	log rank

*** anthracyclin based therapy**

Table S9. Summary and comparison of the clinical features of the 85 patients of the extended cohort (72 AITL and 13 T_{FH}-like PTCL, NOS cases) with (TCR_Mut) or without (TCR_WT) mutations in TCR-related genes (49% vs 51%).

* indicates analysis performed on anthracyclin based treated population

SCT:stem cell transplantation,CR complete response, PR partial response, SD stable disease, PD progressive disease, F: Fisher, MW: Mann Whitney